In vitro-in vivo and cross-life stage extrapolation of uptake and biotransformation of benzo[a]pyrene in the fathead minnow (*Pimephales promelas*)

Chelsea Grimard [a], Annika Mangold-Döring [a,b], Markus Schmitz [c], Hattan Alharbi [d], Paul D. Jones [a,g], John P. Giesy [a,e,f], Markus Hecker [a,g,*], Markus Brinkmann [a,g,h]

[a] *Toxicology Centre, University of Saskatchewan, Saskatoon, Saskatchewan, Canada*
[b] *Institute for Environmental Research (Biology V), RWTH Aachen University, Aachen, Germany*
[c] *Department for Evolutionary Ecology and Environmental Toxicology, Goethe University Frankfurt, Frankfurt, Germany*
[d] *Department of Plant Protection, College of Food and Agriculture Sciences, King Saud University, Riyadh, Saudi Arabia*
[e] *Department of Veterinary Biomedical Sciences and Toxicology Centre, University of Saskatchewan, Saskatoon, Saskatchewan, Canada*
[f] *Department of Environmental Sciences, Baylor University, Waco, Texas, USA*
[g] *School of Environment and Sustainability, University of Saskatchewan, Saskatoon, Saskatchewan, Canada*
[h] *Global Institute for Water Security, University of Saskatchewan, Saskatoon, Saskatchewan, Canada*

ARTICLE INFO

ABSTRACT

Understanding internal dose metrics is integral to adequately assess effects environmental contaminants might have on aquatic wildlife, including fish. *In silico* toxicokinetic (TK) models are a leading approach for quantifying internal exposure metrics for fishes; however, they often do not adequately consider chemicals that are actively biotransformed and have not been validated against early-life stages (ELS) that are often considered the most sensitive to the exposure to contaminants. To address these uncertainties, TK models were parameterized for the rapidly biotransformed chemical benzo[a]pyrene (B[a]P) in embryo-larval and adult life stages of fathead minnows. Biotransformation of B[a]P was determined through measurements of *in vitro* clearance. Using *in vitro-in vivo* extrapolation, *in vitro* clearance was integrated into a multi-compartment TK model for adult fish and a one-compartment model for ELS. Model predictions were validated using measurements of B[a]P metabolites from *in vivo* flow-through exposures to graded concentrations of water-borne B[a]P. Significantly greater amounts of B[a]P metabolites were observed with exposure to greater concentrations of parent compound in both life stages. However, when assessing biotransformation capacity, no differences in phase I or phase II biotransformation were observed with greater exposures to B[a]P. Results of modelling suggested that biotransformation of B[a]P can be successfully implemented into *in silico* models to accurately predict life stage-specific abundances of B[a]P metabolites in either whole-body larvae or the bile of adult fish. Models developed increase the scope of applications in which TK models can be used to support environmental risk assessments.

1. Introduction

Assessments of bioaccumulation are regularly used by toxicologists and environmental professionals to determine risks that water-borne contaminants could pose to aquatic life. While accumulation of a particular chemical might not be an immediate cause for concern, this information is critical for relating the amount of chemical in the exposure medium to that which needs to reach the toxic site of action to elicit adverse responses. Toxicokinetic (TK) *in silico* models allow predicting and quantifying bioaccumulation of chemicals (Nichols et al., 1990; Arnot and Gobas, 2004; Stadnicka et al., 2012; Brinkmann et al., 2016). While traditional TK models are accurate for persistent, neutral, organic chemicals, they do not usually account for biotransformation, which is an essential consideration when determining accumulation of some chemicals as it reduces the overall internal doses of parent materials in bodies of aquatic organisms (McElroy et al., 2011; Carrasco-Navarro

---

et al., 2015; Strobel et al., 2015). The degree of biotransformation is dependent on several biochemical and physiological parameters and, as a result, will naturally differ among life stages and species of fishes.

In vitro techniques have been the predominant methods used for assessing qualitative and quantitative differences in biotransformation of environmental contaminants by characterizing phase I and phase II biotransformation capacity in biological systems (Schlenk et al., 2008; Strobel et al., 2015; Franco and Lavado, 2019). Some of these *in vitro* systems make use of isolated sub-cellular fractions of liver, including microsomes or the post-mitochondrial supernatant fraction (S9), to measure the specificity of substrates and activities relating to a specific phase I or II enzymes under conditions of enzyme saturation (Han et al., 2009; Lee et al., 2014b; Lo et al., 2015). These subcellular fractions can also be used to determine rates of biotransformation under first-order conditions, in relation to a specific substrate (Nichols et al., 2007; Lo et al., 2015; Fay et al., 2017). From these rate constants, *in vitro* intrinsic clearance, which is defined as the volume of blood cleared entirely of a chemical per unit time, can be determined. Recently, the Organisation for Economic Co-operation and Development (OECD) adopted a method for measuring intrinsic clearance using *in vitro* metabolizing systems (OECD 319B; OECD, 2018), which is based on the approach described by Nichols et al. (2006). In combination with *in vivo-in vitro* extrapolation (IVIVE) methods described by Nichols et al. (2013b), the existing *in silico* modeling approaches for bioaccumulation of chemicals in fish could be significantly improved in this way and provide a means of obtaining estimates of hepatic clearance specific to species and chemicals of interest.

Most TK models have been established for adult fishes, while few exist that focus explicitly on early life-stages (ELS) (Foekema et al., 2012). ELS are often considered more sensitive to effects of exposure to some contaminants than their adult counterparts, and are increasingly being used in alternative testing approaches (Embry et al., 2010; Sloman and McNeil, 2012; EFSA, 2015). Understanding life stage-specific TK properties of affecting accumulation of chemicals will be critical to determining and understanding the differences in life stage-specific sensitivity to contaminants. This is particularly relevant for rapidly biotransformed chemicals since biotransformation can act to either detoxify and/or activate a compound. Because ELS fish have been shown to have reduced biotransformation capacity (Knöbel et al., 2012) and use a different proportion of biotransformation pathways (Le Fol et al., 2017) compared to adults, these differences might be of benefit or detriment to the organism. The potential for different outcomes between life stages as a result of differences in chemical biotransformation emphasizes the importance of understanding life stage-specific bio-activation processes. However, even though ELS are shown to be capable of biotransformation at the onset of gastrulation (Otte et al., 2010), due to their small size, obtaining estimates of hepatic clearance directly from the livers of ELS fish is not possible. To address this shortcoming, this study used allometric scaling to obtain estimates of whole-body biotransformation (k_{met}) from measurements of adult hepatic clearance that can be integrated into corresponding TK models.

This study focused on the model chemical, benzo[*a*]pyrene (B[*a*]P), a polycyclic aromatic hydrocarbon (PAH), and a ubiquitous environmental pollutant (U.S. EPA, 2017). B[*a*]P is a known ligand of the aryl hydrocarbon receptor (AhR), and exposure of fish to B[*a*]P has been shown to result in a multitude of effects. B[*a*]P is biotransformed by the enzyme cytochrome P450 1A (CYP1A). CYP1A most often catalyzes detoxification of the parent compound; however, it can also, by reacting with the primary metabolite, generate the highly reactive genotoxic metabolite B[*a*]P-7,8-diol-910-epoxide (BPDE), which can form adducts with DNA and ultimately, result in carcinogenesis (Gelboin, 1980; Hawkins et al., 1990; Stegeman and Lech, 1991; Wang et al., 2010; Yuan et al., 2017). Due to its well-defined biotransformation pathway, B[*a*]P acts as an optimal model compound for evaluation of IVIVE and integration of biotransformation into *in silico* modeling approaches. While a few TK models for B[*a*]P exist for mammals (Crowell et al., 2011;

Heredia-Ortiz et al., 2011), the compound has yet to be integrated into an *in silico* TK model for fish.

To add to the existing database of TK models, the one-compartment bioaccumulation model from Arnot and Gobas (2004) and the multi-compartment physiologically based TK (PBTK) model described by Stadnicka et al. (2012) were adapted to predict accumulation of parent B[*a*]P and production of associated metabolites in embryo-larval and adult life stages of fathead minnows (*Pimephales promelas*), respectively. While *in vitro* clearance of B[*a*]P has been measured in several fishes as listed in the Fish *In Vitro* Biotransformation Database of the European Union Reference Laboratory for Alternatives to Animal Testing (EURL ECVAM) (European Commission, 2018), no values have been reported for fathead minnows. Fathead minnows are one of the most commonly used model species to characterize toxicities of chemicals to both embryo-larval and adult life stages, in addition to having ecological importance (Ankley and Villeneuve, 2006). As such, it is an important target species for development of TK models.

Specific objectives of the present study were to: (a) characterize and compare the *in vitro* transformation kinetics of B[*a*]P at early and adult life stages of the fathead minnow, (b) measure the life stage-dependent relative abundances of B[*a*]P metabolites, (c) apply TK models to extrapolate biotransformation from *in vitro* to *in vivo,* and (d) validate model predictions using data from *in vivo* flow-through exposures to graded concentrations of water-borne B[*a*]P.

2. Materials and methods

2.1. Test organisms

Adult fathead minnows were obtained from an in-house culture originally established from a commercial supplier (Aquatic Research Organisms Inc., Hampton, USA). Fathead minnow embryos were obtained from the same in-house fathead minnow breeding colony. Fish populations were maintained at the Aquatic Toxicology Research Facility (ATRF) at the University of Saskatchewan (Saskatoon, SK, CAN). Husbandry and maintenance details are described in the supplemental materials (Section 1). All fish culture protocols and experimental procedures for both embryo-larval and adult exposures were approved by the Animal Research Ethics Board at the University of Saskatchewan (Protocols #20180052 and #20160090).

2.2. Waterborne B[a]P exposures

Waterborne chronic exposures to B[*a*]P were conducted to evaluate uptake by and biotransformation of B[*a*]P in the embryo-larval and adult life stages of fathead minnows. Nominal concentrations for both exposures were 1.3, 4.0 or 12.0 μg B[*a*]P/L (benzo[*a*]pyrene, Sigma-Aldrich, Oakville, ON, CAN) using 0.02 % DMSO ($\geq$ 99.9 % dimethyl sulfoxide, Fisher Scientific Co., Ottawa, ON, CAN) as the carrier solvent, or 0.02 % DMSO only as the solvent control. The embryo-larval exposure also included de-chlorinated ATRF water as the water control. Due to space limitations and size of the exposure experiment, a water control was not included in the adult fathead minnow experiment. The exposure concentrations were chosen to represent both an environmentally relevant exposure concentration below the water solubility threshold (*i.e.* 3.8 μg B[a]P/L) (Miller et al., 1985), as well as concentrations above water solubility that was expected to induce a response (*i.e.*, changes enzyme activity, gene expression, morphometrics, behavior, and survival) (Gravato and Guilhermino, 2009; Costa et al., 2013; Lee et al., 2014a; Booc et al., 2014). In the first experiment, fathead minnow embryos (<10 h post-fertilization) were exposed for 32 days. Whole-body samples were taken after three, seven, 14 and 32 days of exposure. In the second experiment, adult fathead minnow breeding groups consisting of two males and three females were exposed for 21 days. Whole liver and gall bladder (bile) samples were taken after four, seven, 14 and 21 days of exposure. Sampling points were chosen to

characterize the uptake of B[*a*]P, and in the case of the embryo-larval exposure, sampling points also characterized important developmental stages, *i.e.*, the early embryo, 0–3 days post fertilization (dpf), the yolk-sac, 3–7 dpf, and the free-feeding stage, 7–32 dpf. In both experiments, respective samples were also taken after a seven-day depuration period to characterize the elimination of B[*a*]P. Exposure details are provided in the supplementary materials (Section 2).

2.3. Sample collection

Whole-body larvae were sampled on days three, seven, 14 and 32 of exposure, as well as after the depuration period. Larval samples were taken on days three (20 larvae; *n* = 2 per treatment/endpoint) and seven (10 larvae; *n* = 2 per treatment/endpoint), and were pooled to increase tissue mass for biochemical assays. Samples on day 14 were taken in pooled groups of two individuals for biochemical (*n* = 3 per treatment), chemical (*n* = 2 per treatment) and lipid analysis (*n* = 2 per treatment). On day 32 and after the depuration period, larvae were sampled in pooled groups of five or three larvae, respectively, for biochemical (*n* = 5 per treatment), chemical (*n* = 5 per treatment) and lipid analysis (*n* = 5 per treatment). At each sampling point, wet mass was recorded. Samples were immediately flash-frozen in liquid nitrogen and stored at −80 °C until further analysis.

Adult fish were euthanized rapidly by blunt force trauma to the head on day four (*n* = 5 per treatment), seven (*n* = 2 per treatment), 14 (*n* = 2 per treatment), and 21 (*n* = 5 per treatment) of exposure, as well as after the depuration period (*n* = 2 per treatment). The wet mass was recorded for each fish. Liver samples were taken for biochemical analysis and gall bladder (bile) for chemical analysis of B[*a*]P metabolites. Samples were immediately flash-frozen in liquid nitrogen and stored at −80 °C until analysis.

2.4. Analytical confirmation of aqueous B[*a*]P and B[*a*]P metabolites

Samples of aqueous B[*a*]P were collected on day one, 15, and 30 of the embryo larval exposure, and on days two, 11 and 20 of the adult exposure. Sampling times were chosen to assess aqueous B[*a*]P concentrations at the start, middle and end of exposures. Water samples (1 L) were sent to SGSS AXYS Analytical Services Ltd. (Sydney, BC, CAN) for quantification of B[*a*]P (SGS AXYS method MLA-021) using gas chromatography-mass spectrometry (GC–MS) following C18 solid-phase extraction (SPE). B[*a*]P D-12 was used as an internal standard with a recovery of 39–81 %. Matrix spike samples exhibited recoveries of 101–102 %. Lab blanks tested negative for B[*a*]P.

The protein precipitation method described by Nacalai Tesque, Inc. (2017) was used to quantify metabolites of B[*a*]P. Whole-body embryos were homogenized in HPLC grade acetonitrile (ACN, Fisher Scientific Co., Ottawa, ON, CAN) for 20 s at a ratio of 1:10 (m/v), while gall bladder (bile) samples were homogenized in ACN for 20 s at a ratio of 1:100 (m/v). Samples were incubated on ice for 15 min and then centrifuged at 1700 × g for 15 min. The supernatant subsequently sampled for quantification of metabolites.

The major metabolites 3-hydroxy-benzo[*a*]pyrene (OH-B[*a*]P) and 3-hydroxy-benzo[*a*]pyrene *O*-glucuronide (gluc-B[*a*]P) were quantified using ultra-high-performance liquid chromatography high-resolution mass spectrometry (UPLC-HRMS) by use of a modified method described by Beach et al. (2000); Zhu et al. (2008); Lu et al. (2011), and Tang et al. (2016). Metabolite analysis was conducted using a Vanquish UHPLC and Q-Exactive™ HF Quadrupole-Orbitrap™ mass spectrometer (Thermo-Fisher, Waltham, MA, USA). Samples were ionized in negative mode heated electrospray ionization (HESI) followed by a full MS/parallel reaction monitoring (PRM) method. Concentrations of OH-B[*a*]P were quantified directly using analytical standards and external calibration. To quantify gluc-B[*a*]P, a semi-quantitative method was used in which peak areas of from the OH-B[*a*]P standard curve were converted to gluc-B[*a*]P peak areas using response factors. The detailed method is described in the supplementary materials (Section 3).

Final concentrations of B[*a*]P metabolites, reported as ng/mg whole body larvae or bile, were calculated from the volume of solvent used for extraction and specific bile mass. B[*a*]P equivalents, *i.e.*, mass concentrations that are independent of differences in molecular mass of the parent compound and the two metabolites, were calculated from the obtained metabolite concentrations for use in subsequent analyses and to match model output units.

2.5. Measurement of intrinsic clearance

Intrinsic clearance (*n* = 2) in fathead minnow liver tissue was measured using an adaptation of OECD 319B: Determination of *in vitro* clearance using rainbow trout liver S9 sub-cellular fraction (RT-S9) (OECD, 2018). Pooled liver tissue was homogenized in 5 μL homogenization buffer per mg tissue and centrifuged at 9000 × g for 20 min. The supernatant (S9) was sampled for use in the *in vitro* clearance assay. Assay details are described in the supplementary material (Section 4). Depletion of parent B[*a*]P from the S9 was measured at 0, 20, 40, 60, 80, 100 and 120 min by use of synchronous fluorescence spectrophotometry in a quartz cuvette (Lumina, Thermo Fisher Scientific, Ottawa, ON, CAN). Concentrations of B[*a*]P at each time point were determined from a standard curve and concentrations were plotted as a function of time. The depletion curve was *log*-transformed, and the first-order depletion rate constant (*k*) was determined by multiplying the slope of the line by -2.3. Intrinsic clearance (Cl$_{int, \, in \, vitro}$) was calculated (Eq. 1):

$$Cl_{int, \, in \, vitro}(mL \; h^{-1} mg^{-1}) = \frac{k(h^{-1}) \cdot volume \; of \; the \; reaction \; (mL)}{reaction \; protein \; concentration \; (mg \; L^{-1})} \quad (1)$$

2.6. Biochemical analysis

EROD (7-ethoxyresorufin *O*-deethylase) and GST (glutathione-*S*-transferase) activities were measured to characterize phase I and II biotransformation as described by Kennedy and Jones (1994) and Habig et al. (1974), respectively, with modifications. For both assays, the post-mitochondrial supernatant fraction was generated from whole-body larval and adult liver samples following a modified OECD 319B protocol (OECD, 2018). Tissue was homogenized in homogenization buffer at a ratio of 20 μL buffer: 1 mg tissue then centrifuged at 10, 000 × g. The supernatant was subsequently taken for use in biochemical assays. EROD activity (pmol/mg/min; *n* = 5) was measured through fluorescent measurements of resorufin (570 nm excitation/ 630 nm emission) and protein (365 nm excitation/ 480 nm emission). GST activity (nmol/mg/min; *n* = 5) was measured through a kinetic measurement of CDNB (1-Chloro-2,4-dinitrobenzene; 340 nm emission). Assays are described in detail in the supplementary materials (Sections 5 and 6).

2.7. Lipid analysis

Total whole-body lipid content in both life stages was quantified using a modification of the microcolorimetric sulfophosphovanillin (SPV) method described by Lu et al. (2008). Lipids (*n* = 5) were extracted using whole-body fish (embryo-larval, 10−50 mg wet mass; adult, 10−50 mg homogenized sub-sample). Lipid extracts were quantified by the addition of sulphuric acid and SPV reagent. Lipid content (mg) was determined through measurements of absorbance and lipid percent was subsequentially calculated. Additional assay details are provided in the supplementary materials (Section 7).

2.8. Estimation of embryo-larval cardiac output

Cardiac output was determined for fathead minnow larvae to use in *in vitro-in vivo* scaling calculations of whole-body biotransformation rates using an Excel spreadsheet provided by Nichols et al. (2013b) for

subsequent use in *in silico* models (summarized in supplemental materials). Adult fish cardiac output was not measured since it has been calculated previously (Stadnicka et al., 2012). Cardiac output was measured at three, seven, and approximately 32 days post fertilization (dpf) by use of methods described by Schwerte et al. (2005). Larvae ($n = 5$) were anesthetized by use of Aquacalm™ (approximately 200 µg/L, Syndel; Nanaimo, BC, CAN) and heart rate (beats per minute) was manually counted for two minutes. The heart was imaged using digital microscopy (ZEISS Observer Z.1 equipped with Axiocam 105, Carl Zeiss Canada, Toronto, ON) and the length and width of the ventricle were recorded four times for both the diastole and systole phases. The ventricular volume for each phase ($4/3 * \pi * \text{length} * \text{width}^2$) was calculated and used to determine stroke volume (diastole volume – systole volume) and cardiac output (stroke volume * heart rate).

2.9. TK models

The current study provided parameters to be used in an embryo-larval one-compartment TK and adult multi-compartment TK model for fathead minnows (detailed in supplemental materials Section 8 and 9). For the embryo-larval model, the whole-body biotransformation rate was calculated by scaling adult *in vivo* intrinsic clearance by use of measurements of embryo-larval cardiac output. The adult model used the *in vivo* intrinsic clearance directly to calculate hepatic clearance, which was applied to determine metabolite abundance in the bile. Both models used measurements of wet mass and whole-body lipid content as inputs. Additionally, the adult model used measurements of bile mass. The models were used to make predictions of metabolite abundance, in either the whole-body (embryo-larval) or the bile (adult), which were compared to results determined by the chemical analysis of whole-body or bile metabolite abundance, respectively. Model outputs for all compartments, including the bile, were produced as parent B[*a*]P concentration units. Therefore, for the purpose of evaluating model accuracy and to replicate model units, the measured concentrations of B[*a*]P metabolites, OH-B[*a*]P and gluc-B[*a*]P, were converted to B[*a*]P equivalents and summed (ng mg whole body tissue^{-1}, ng mg bile^{-1}).

2.10. Statistical analysis

A parametric analysis consisting of a 2-way ANOVA followed by Tukey's HSD post hoc test was used to determine if differences existed among treatment groups and time of exposure for chemical analysis of B[*a*]P metabolites, EROD, and GST activity. The two-sided Iglewicz and Hoaglin's robust outlier test ($Z = 3.5$) was used to detect multiple outliers (Contchart online calculator; Contchart Software, 2018). Data were log-transformed when necessary to meet heteroscedasticity (Spearman's test for heteroscedasticity) and normality assumptions. A Wilcoxon sign test was performed to determine if differences existed between measured and predicted B[*a*]P equivalent values. Significant differences were defined by $p \leq 0.05$. All statistical tests were performed using GraphPad Prism 8® (GraphPad Software, Inc., San Diego, CA, USA). Additionally, RMSE (root mean square error) calculations were performed to analyze model accuracy. All RMSE calculations were performed by use of Microsoft® Excel 16.30 (Microsoft Co., Redmond, WA, USA).

3. Results

3.1. B[*a*]P concentrations

Mean ($\pm$ S.D.), measured aqueous concentrations of B[*a*]P for the embryo-larval exposure were 0.16 ($\pm$ 0.15), 0.85 ($\pm$ 0.70) and 4.55 ($\pm$ 3.18) µg B[*a*]P/L. For the adult life stage exposure, mean, measured aqueous concentrations of B[*a*]P ($\pm$ S.D.) were 0.03 ($\pm$ 0.01), 0.08 ($\pm$ 0.02) and 1.34 ($\pm$ 0.70) µg B[*a*]P/L. Time-resolved concentrations are stated in supplemental figure S5. The measured concentrations were considerably lower than nominal concentrations. Losses of B[*a*]P are likely a result of sorption to the exposure aquaria and particulates (*i.e.*, food and algae), incomplete solubility, and degradation. At these measured concentrations, no significant effect on growth, reproduction or survival were observed.

3.2. Chemical analysis of B[*a*]P metabolites

A significant interaction occurred between duration and magnitude of exposure to B[*a*]P for concentrations of OH-B[*a*]P metabolite in both the embryo-larval (2-way ANOVA, df = 16, $F_{16,45} = 6.294$, $p < 0.0001$) and adult life stage (2-way ANOVA, df = 12, $F_{12,40} = 9.916$, $p < 0.0001$) (Fig. 1). Likewise, a significant interaction also occurred for gluc-B[*a*]P between concentration and duration of exposure in both the embryo-larval (2-way ANOVA, df = 16, $F_{16,47} = 6.811$, $p < 0.0001$) and the adult life stage (2-way ANOVA, df = 12, $F_{12,40} = 9.119$, $p < 0.0001$) (Fig. 1). In the embryo-larval stage significant differences among durations of exposure suggested an increase in the abundance of both OH-B[*a*]P and Gluc-B[*a*]P with increasing exposure time. A slight decrease in both metabolites, however, was observed after 14 days of exposure. This trend was less apparent in the adult life stage, in which differences in abundances of OH-B[*a*]P varied among exposure times in the 0.03 and 0.08 µg B[*a*]P/L treatments. Similar to the embryo-larval stage, an increasing trend in the abundance of OH-B[*a*]P among exposure time was observed in the highest exposure treatment (1.34 µg B[*a*]P/L). Differences in the abundances of Gluc-B[*a*]P, however, varied among all exposure times for all B[*a*]P treatments in the adult exposure.

Abundances of B[*a*]P equivalents (mass concentrations that are independent of differences in molecular mass of the parent B[*a*]P and the two metabolites) used for evaluating model accuracy are shown in the supplemental materials (Supplemental Figure S1).

3.3. Enzyme activity analysis

No significant differences in EROD activity occurred among treatment groups for either life stage. There was, however, a significant difference in EROD activity among exposure days for both the embryo-larval (2-way ANOVA, df = 2, $F_{2,40} = 81.00$, $p < 0.001$; Fig. 2A) and adult life stage (2-way ANOVA, df = 2, $F_{2,58} = 8.565$, $p = 0.0006$; Fig. 2B). In the embryo-larval stage the difference among exposure times indicated a decrease in EROD activity, while in the adult stage, differences among treatments suggest a slight increase in EROD activity over the duration of the exposure.

Similarly, there were no significant differences in GST activity in the embryo-larval stage among exposure concentrations, but a significant difference among durations of exposure was observed (2-way ANOVA, df = 2, $F_{2,40} = 81.00$, $p < 0.0001$; Fig. 3A). These differences suggest an increase in GST activity in the embryo-larval stage over the duration of the exposure. In the adult life stage, a significant interaction for GST activity occurred between magnitude and duration of exposure to B[*a*]P (2-way ANOVA, df = 6, $F_{6,60} = 2.582$, $p = 0.0272$; Figure B). The differences in the adult stage, however, were highly variable and did not indicate either induction or inhibition of GST activity with B[*a*]P exposure.

3.4. TK model parameters and outputs

Parameters specific to exposures are summarized (Table 1). Additional model parameter values are defined in the supplemental materials (Supplemental Table S2, Supplemental Table S3). A significant correlation between predicted and measured internal concentrations of B[*a*]P equivalents was observed for both the embryo-larval and adult models (Fig. 4). Model outputs were within approximately one order of magnitude of the measured values (Fig. 4, Fig. 5). No significant differences were observed between predicted and measured values for either model (embryo-larval one-compartment, Wilcoxon Signed Rank

A

B
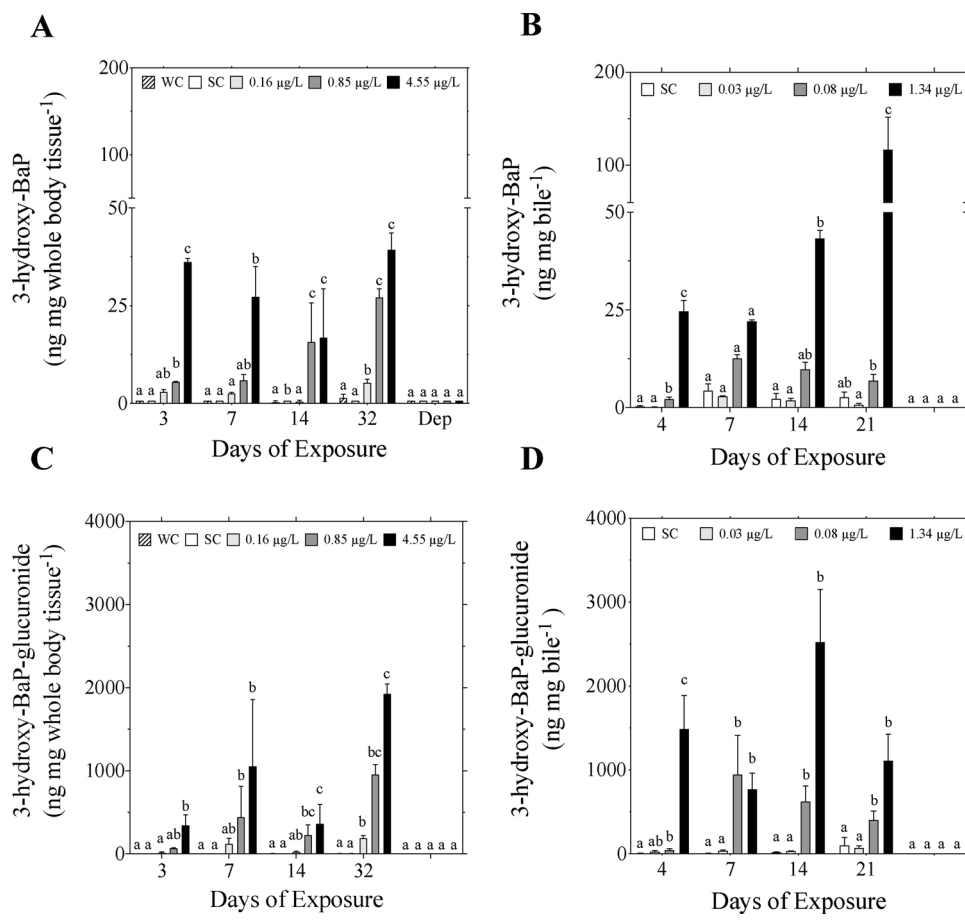
Fig. 1. Abundances of 3-hydroxy-B[*a*]P and 3-hydroxy-B[*a*]P glucuronide (ng mg whole body tissue^{-1} or ng mg bile^{-1}) in whole body embryo-larval (A, C) or the bile of adult (B, D) fathead minnows after three, seven, 14 and 32 or four, seven, 14 and 21 days of exposure, respectively, to increasing concentrations of B[*a*]P as well as water control (WC) and solvent control (SC). Data is expressed as mean ± standard error of the mean (S.E.M.). Different letters denote a significant difference in B[*a*]P metabolites among treatment groups within each respective time point (2-way ANOVA with Tukey's HSD, $\alpha = 0.05$).

C

D

A

B
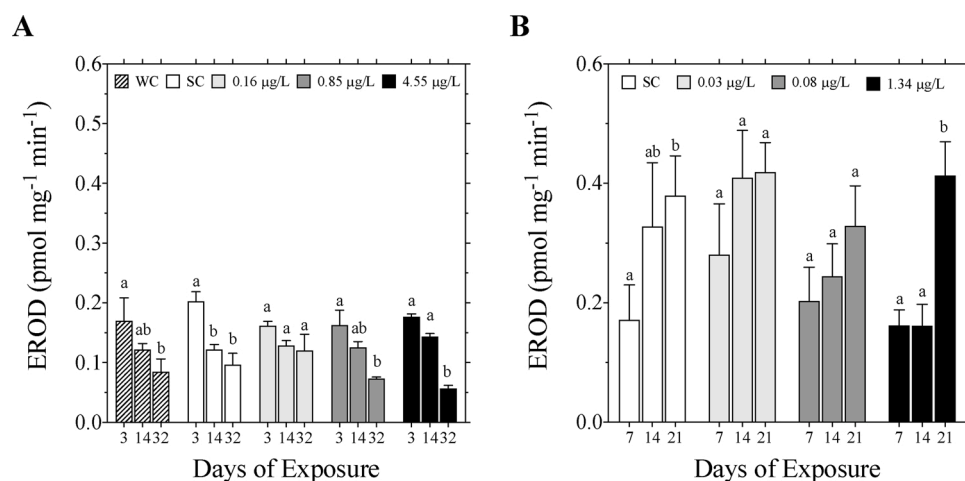
Fig. 2. EROD activity (pmol mg^{-1} min^{-1}) for whole body embryo-larval (A) or liver of adult (B) fathead minnows after three, 14, and 32 or seven, 14 and 21 days of exposure, respectively, to increasing concentrations of B[*a*]P as well as water control (WC) and solvent control (SC). Data is expressed as mean ± S.E.M. Different letters denote a significant difference in EROD activity among time points within each respective treatment group (2-way ANOVA, $\alpha = 0.05$). No significant differences existed among treatment groups within each respective time point.

test; $p = 0.3013$; Adult multi-compartment, Wilcoxon Signed Rank test; $p = 0.9697$). The adult model, however, had a slightly smaller RMSE of 0.6010 log units, compared to the embryo-larval one-compartment model with an RMSE of 0.6371 log units.

4. Discussion

Using *in silico* models is a promising approach that enables prediction of the internal dose metrics for a growing number of fish species, chemicals, and exposure scenarios. In this study, we investigated the biotransformation characteristics and capacity in embryo-larval and

adult life stages of fathead minnow exposed to water-borne B[*a*]P. These data were further integrated into pre-existing models. Results showed that the resulting models were successful in predicting the life-stage specific abundances of B[*a*]P metabolites in both the embryo-larval and adult life stages of fathead minnow.

4.1. Integration of biotransformation into TK models

The finding of no differences in either phase I (CYP1A; EROD) or phase II (glutathione; GST) enzyme activities observed among treatments for both life stages of fathead minnow (Fig. 2, Fig. 3) is consistent

A

B
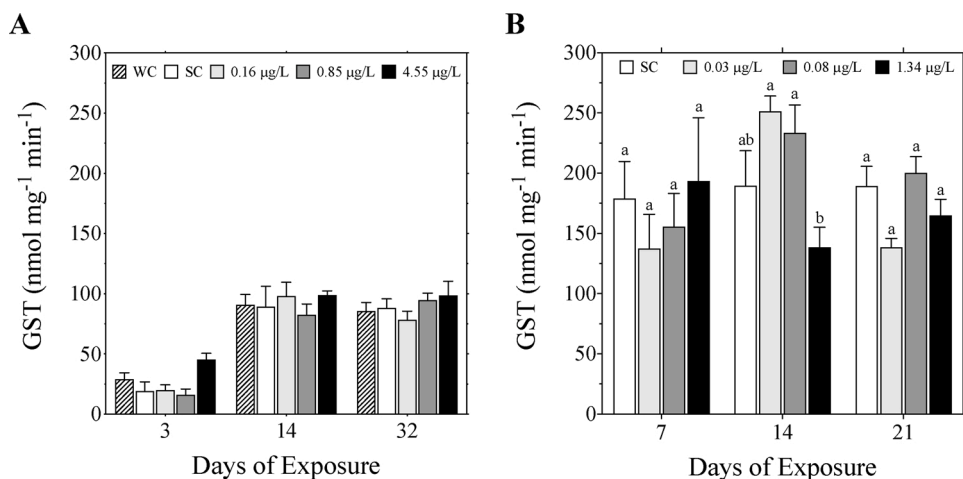
Fig. 3. GST activity (nmol mg^{-1} min^{-1}) for whole body embryo-larval (A) or liver of adult (B) fathead minnows after three, 14, and 32 or seven, 14 and 21 days of exposure, respectively, to increasing concentrations of B[a]P as well as water control (WC) and solvent control (SC). Data is expressed as mean ± S.E.M. Different letters denote a significant difference in GST activity among treatment groups within each respective time point (2-way ANOVA, α = 0.05). No significant differences existed in the embryo-larval life stage among treatment groups for each respective time point.

Table 1

Measured input parameters for embryo-larval (ELS) one-compartment and adult multi-compartment models.

| Life stage	Wet mass (mg ± S.D.)	Bile volume (mg ± S.D.)	Cl$_{int, in vitro}$[b] (ml/h/mg)	Lipid (%)	Cardiac output (nl/min ± S.D.)	K$_{MET}$[c] (1/d)
ELS 3 dpf[a]	1.22 ± 0.17	—	—	1.84 ± 0.52	29.64 ± 9.62	1.325
ELS 7 dpf	0.79 ± 0.11	—	—	1.70 ± 0.41	60.82 ± 18.71	2.748
ELS14 dpf	3.60 ± 1.76	—	—	2.30 ± 0.84	interpolated[e]	interpolated[e]
ELS 32 dpf	35.00 ± 8.00	—	—	2.84 ± 1.16	955.25 ± 168.96	0.905
Adult day 4	2248 ± 1386	6.23 ± 3.81	0.742 ± 0.061	—	calculated[d]	—
Adult day 7	2337 ± 1440	4.74 ± 2.73	0.742 ± 0.061	—	calculated[d]	—
Adult day 14	2396 ± 1418	4.27 ± 2.56	0.742 ± 0.061	—	calculated[d]	—
Adult day 21	2481 ± 1421	4.12 ± 2.60	0.742 ± 0.061	—	calculated[d]	—

[a] days post fertilization (dpf).
[b] intrinsic *in vitro* clearance (Cl$_{int, in vitro}$).
[c] whole body biotransformation rate (K$_{MET}$).
[d] value as determined from fathead minnow TK model outlined in Stadnicka et al. (2012).
[e] interpolated using ELS one-compartment model.
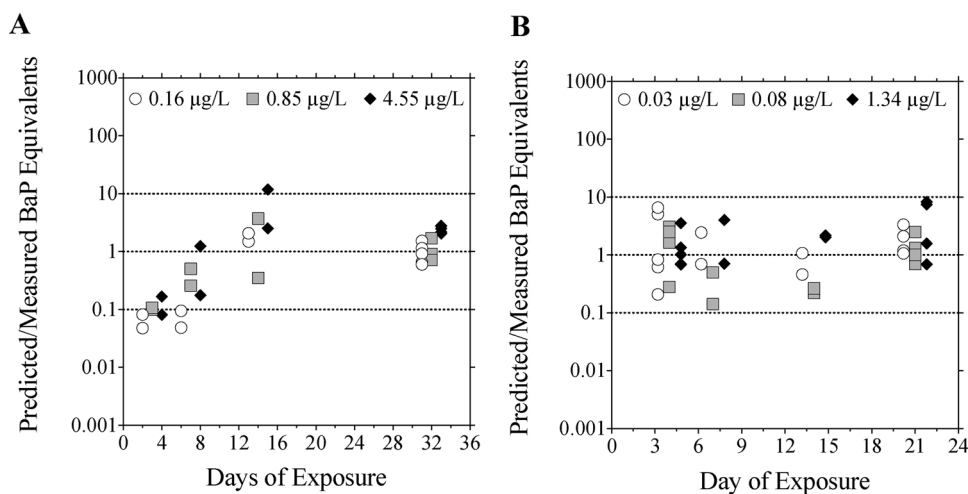
A

B
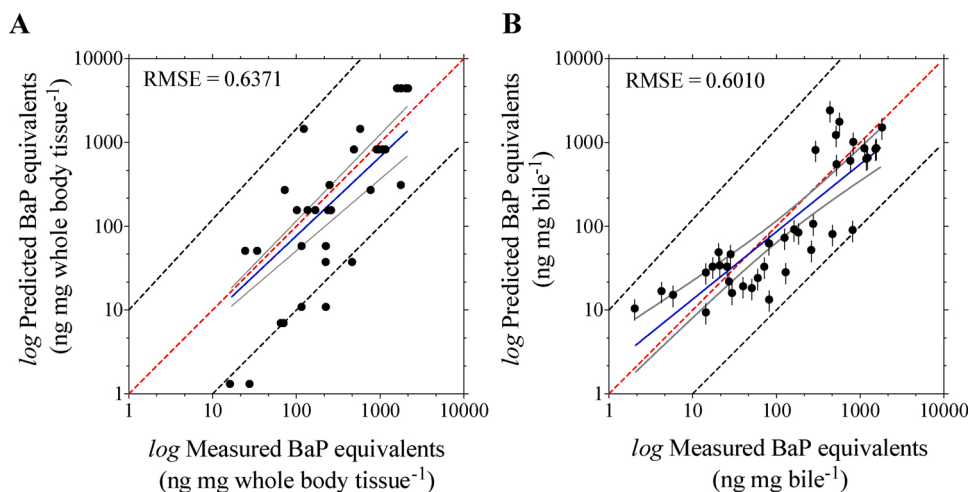
Fig. 4. Relationships between predicted and measured concentrations of B[a]P equivalents from the embryo-larval one compartment (A) and adult multi-compartment (B) model outputs with linear regression (blue) and associated 95 % confident intervals (grey), equality line (dashed red) and ± 10-fold deviation from equality (dashed black). Error bars for the adult multi-compartment model points indicate range of predictions in the last eight hours of simulation to depict bile dynamics. Predicted B[a]P equivalents were obtained directly from model outputs. Measured B[a]P equivalents were calculated as mass concentrations that are independent of differences in molecular mass of the parent B[a]P and the two metabolites, OH-B[a]P and gluc-B[a]P, from measured metabolite concentrations in order to match model output units. RMSE, root mean squared error.

with data published from previous aqueous B[a]P studies in other fishes, which revealed that induction of these responses is not commonly found in fish unless exposed to B[a]P concentrations of 10 μg B[a]P/L or greater (Sandvik et al., 1997; Peters et al., 1997; Ortiz-Delgado et al., 2007; Costa et al., 2011). Measured, aqueous B[a]P concentrations from this study were substantially lesser. Additionally, it has been suggested that cyprinids, such as the fathead minnow, exhibit lesser CYP1A activity and inducibility compared to other species, and accordingly show fewer effects such as carcinogenesis (Hawkins et al., 1991; van den Hurk

et al., 2017). However, given these results, the *in vitro* clearance of B[a]P in fathead minnow (Table 1) was within the range of values that have previously been measured in other species such as *Oncorhynchus mykiss* (rainbow trout) and *Lepomis macrochirus* (bluegill sunfish) as listed in EURL ECVAM *In Vitro* Biotransformation Database (European Commission, 2018).

Biotransformation of substrates typically follows the Michaelis-Menten model, which contains a first-order and a quasi zero-order, *i.e.*, saturation phase. It is important to consider the possibility of

A

B

Fig. 5. Relationships between predicted and measured concentrations of B[a]P equivalents from the embryo-larval one compartment (A) and adult multi-compartment (B) model outputs relative to the day of exposure with ± 10-fold error from equality (grey). Predicted B[a]P equivalents were obtained directly from model outputs. Measured B[a]P equivalents were calculated as mass concentrations that are independent of differences in molecular mass of the parent B[a]P and the two metabolites, OH-B[a]P and gluc-B[a]P, from measured metabolite concentrations in order to match model output units.

saturation kinetics when integrating biotransformation into TK models as it could have a substantial impact on their scaling, and subsequently, model outputs. The concept of enzyme saturation regarding B[a]P exposure was explored by Nichols et al. (2013a). However, it was concluded that, in contrast with other chemicals, at a high exposure concentration (0.98 μM) saturation was unlikely, and would have little or no impact on hepatic clearance of B[a]P, but rather hepatic clearance was more sensitive to liver perfusion rates due to the high extraction ratio of B[a]P.

The information provided by Nichols et al. (2013a), along with the insignificant differences we observed in phase I and II biotransformation, provided a basis for the assumption that all exposure concentrations occurred within the first-order portion of the Michaelis-Menten model. This assumption meant that biotransformation would increase proportionally with our increase in exposure concentrations. Therefore, we were able to apply a single biotransformation parameter for all exposure simulations and did not account for saturation kinetics. In exposure scenarios where saturation kinetics could occur, a series of clearance studies would need to be performed as described by Nichols et al. (2013a).

4.2. Model performance and predictive power

Integration of biotransformation into pre-existing TK models produced accurate predictions within 10-fold of measured concentrations for both the embryo-larval and adult life stages of fathead minnow (Fig. 4). The one-compartment embryo-larval model showed slightly lesser predictive power compared to the multi-compartment adult model. This result is consistent with previously published results for when these two model types were compared (Nichols et al., 2007, Stadnicka et al., 2012). Inaccuracies in model predictions from the one-compartment model occurred specifically during the first two phases of development, i.e. the egg stage (0–3 dpf) and yolk sack stage (3–7 dpf) and became less prevalent as the model progressed into the free-feeding stages (7–32 dpf) (Fig. 5A). These inaccuracies are potentially a result of estimates of biotransformation for the embryo-larval fish that was allometrically scaled from measurements of adult in vitro clearance rates using measurements of cardiac output. Measurements of embryo-larval stage-specific in vitro clearance were attempted using the methods described in OECD 319B (OECD, 2018); however, the assay was not optimized for use with whole-body samples and measurements could not be obtained due to insufficient sensitivity. This was likely a result of enzyme protein dilution within the whole-body larvae, and therefore, a sufficient concentration of enzymes could not be isolated for proper performance in the assay.

Few studies have been conducted in which embryo-larval

biotransformation was compared to adults. Studies conducted with embryo-larval zebrafish have shown that biotransformation can begin as early as the gastrulation stage of development (Otte et al., 2010), and that larvae are capable of extensive phase II biotransformation as soon as 3 dpf (Le Fol., 2017). Therefore, these results suggest that the embryo-larval fish have a higher capacity for biotransformation than we calculated during the initial stages of embryo-larval development. This conclusion is supported by the observed linear relationship between whole-body biotransformation (k_{met}) and B[a]P equivalent concentrations (Supplemental Figure S2C). The positive relationship indicates that increases in k_{met} will generate increases in B[a]P equivalents. Additional research pertaining to the optimization of in vitro clearance assays for embryo-larval stages of fish would provide more accurate estimates of biotransformation to be used in embryo-larval stage TK models.

Performance of the adult multi-compartment model, with an RMSE of 0.60 log units (Fig. 4B), were comparable to previously published results when the model was used for exposure simulations across numerous other chemicals in the fathead minnow, which showed an RMSE of 0.66 log units (Stadnicka et al., 2012; Brinkmann et al., 2016). Advances to the existing TK model for fathead minnows were made by the addition of a bile compartment, which included the parameters bile flow, volume, and purge time, to depict bile dynamics and include biotransformation. A similar TK model including bile dynamics for rainbow trout has been described by Brinkmann et al. (2014). Additionally, we were able to make bile-specific predictions of metabolites, allowing for a simple quantification method of B[a]P metabolites in the bile to act as a validation data set. Some assumptions needed to be made regarding the bile specific parameters as literature values and measurement techniques were not available. Changes in these parameters were shown to influence the abundance of metabolites predicted, and therefore, species-specific measurements of these parameters could change model performance (Supplemental Figure S2E, F).

An additional assumption implemented into the adult multi-compartment model was that only 60 % of the metabolites predicted would represent OH-B[a]P and gluc-B[a]P. This assumption was made based on studies conducted with mummichog (Fundulus heteroclitus) in which the abundance of OH-B[a]P and the associated glucuronide was determined to be between 58–66 % of total metabolites produced (Zhu et al., 2008). Measuring the specific concentrations of all B[a]P metabolite fractions produced by fathead minnows could further improve model performance. In the embryo-larval model, 100 % of the predicted metabolites were assumed to be the OH-B[a]P and associated glucuronide as studies conducted with zebrafish larvae suggest that embryo-larval biotransformation occurs predominately through the glucuronide pathway opposed to a combination of other pathways such as sulfation (Le Fol et al., 2017). In both life-stages, however, it should

be noted that other pathways of B[*a*]P biotransformation might exist. These pathways include hydrolysis *via* the epoxide pathway to form the genotoxic metabolite BPDE, conjugation *via* GST, and the formation of diols, diones, tetrols, triols, phenols and quinones (Gelboin, 1980; Kennedy and Tierney, 2008; Zhu et al., 2008; Liu et al., 2014; Strobel et al., 2015).

Biotransformation was also shown to affect abundances of B[*a*]P metabolites produced (Supplemental Figure S2D). However, at greater rates of biotransformation, the sensitivity of the parameter was shown to decrease. This further indicates that the extent of metabolites produced from hepatic clearance of rapidly metabolized chemicals is largely influenced by liver perfusion rather than binding to CYP proteins and enzyme activity. Studies conducted with isolated perfused rainbow trout livers showed similar findings (Nichols et al., 2009; Nichols et al., 2013). In these studies, the effect of increasing BSA concentration in the liver perfusate on hepatic clearance was evaluated. For chemicals with high extraction ratios, such as B[*a*]P and pyrene, changes in protein concentration had little effect on hepatic clearance. No evidence of enzyme saturation was observed, and therefore, biotransformation capacity was determined to be relative to rate of liver perfusion (Nichols et al., 2013a). However, for the chemicals naphthalene, fluorene, anthracene, phenanthrene (Nichols et al., 2013b) and 7-ethoxycoumarin (Nichols et al., 2009), decreases in BSA concentration resulted in increases in hepatic clearance suggesting that protein binding has greater influence on hepatic clearance for these compounds. These differences among chemicals are attributed to their respective log K_{ow} values, as log K_{ow} was shown to have a positive correlation with *in vitro* clearance (Nichols et al., 2013). In mammals, it has been shown that CYP1A enzymes have a higher affinity for hydrophobic compounds (Long and Walker, 2003). Therefore, it is likely that the greater the hydrophilicity of a chemical (*i. e.*, naphthalene, fluorene, anthracene, phenanthrene, and 7-ethoxycoumarin) the greater its affinity for non-CYP proteins. As protein content decreases the availability for these chemicals to bind to CYP enzymes increases, resulting in increased *in vitro* clearance. For more hydrophobic chemicals such as B[*a*]P and pyrene, there is a higher affinity for CYP enzymes compared to non-CYP proteins, and changes in protein content have no effect on *in vitro* clearance.

4.3. Differences between life stages

Differences in the biotransformation characteristics between life stages were observed. The embryo-larval life stage exhibited lesser formation of B[*a*]P metabolites compared to the adult life stage (Fig. 1). This difference, however, was difficult to quantify based on results of this study, as B[*a*]P equivalents were measured in the whole body of the embryo-larval stage while in the adult stage they were assessed in bile. Therefore, some dilution of metabolites likely occurred in the whole-body embryo-larval samples corresponding to the reduced abundance of B[*a*]P metabolites. The same conclusion can be drawn for the differences in EROD and GST activity between life stages (Fig. 2, Fig. 3). However, differences in metabolic capacity between life stages of fish have been observed previously. Knöbel et al. (2012) found that when embryo-larval and adult zebrafish were exposed to allyl alcohol, a chemical for which biotransformation is responsible for the associated toxicity, embryo-larval fish exhibited a LC$_{50}$ value 1059-fold greater than the adult fish. This difference was attributed to a lack in the biotransformation capacity at the embryo-larval stage, and as a result a lesser concentration of toxic metabolites was produced compared to adult fish. Le Fol et al. (2017) also demonstrated life stage-specific differences in metabolic capacity when embryo-larval and adult zebrafish were exposed to benzophenone-2 (BP2) and bisphenol S (BPS). Overall, the adult life stage showed a greater capacity of biotransformation for both chemicals. Additionally, for BP2, life stage differences in metabolic pathways were observed. Glucuronidation was the predominant pathway in the embryo-larval stage while sulfation predominated in the adult life stage. Understanding these life stage differences is critical

when assessing toxicity for chemicals that are activated by biotransformation. If life stage-specific biotransformation is not considered, researchers and risk assessors might underestimate the toxic effects of such chemicals.

The concentration of a chemical that can reach the target site of action is known to be influenced directly by biotransformation activity (McElroy et al., 2011; Carrasco-Navarro et al., 2015; Strobel et al., 2015). B[*a*]P is a known ligand for the AhR, inducing the transcription of target genes, and ultimately the CYP1A and CYP1B proteins responsible for biotransformation of parent B[*a*]P into toxic metabolites (Gelboin, 1980). The results of this study suggest that the embryo-larval stage will be less affected by genotoxicity from biotransformation of B[*a*]P compared to the adult life stage. However, the embryo-larval stage, in turn, might be more susceptible to other effects associated with binding of the AhR such as teratogenicity (Jönsson et al., 2007; Schiwy et al., 2015). Developmental effects, likely associated with AhR ligand binding in the embryo-larval stage, have been shown to be directly related to increases in aqueous B[*a*]P exposure concentrations (Gravato and Guilhermino, 2009). These results emphasize the importance of life stage-specific models parameterized for chemicals that are rapidly biotransformed for accurate risk assessments for fish.

The use of ELS of fish in support of toxicity studies and hazard assessments is increasing. ELS are often considered to be more sensitive to contaminants than adults. However, as discussed above, ELS might be less sensitive to exposure to some chemicals in which biotransformation elicits toxicity, as the ELS were shown to have less extensive biotransformation capacity compared to the adult life stage. Therefore, a greater understanding of contaminant effects on ELS is important in terms of protection of species survival and ecosystem homeostasis. Additionally, the embryo-larval stage is currently being considered as a replacement and refinement method to live animal testing (EFSA, 2005). Thus, a better understanding of life-stage specific differences in toxicokinetic processes is essential in advancing these developments. Research initiatives such as the fish embryo test (FET) (Lammer et al., 2009; Embry et al., 2010; Knöbel et al., 2012; OECD, 2013; Kais et al., 2017), the embryo test with the Zebrafish *Danio rerio* (DarT) (Nagel, 2002), and the EcoToxChip project focusing on fish, amphibian and bird embryo testing (Basu et al., 2019) are currently using embryo-based approaches as a replacement for juvenile or adult organisms, and will benefit greatly from more accurate internal exposure predictions. Additionally, ELS tests as well as *in silico* approaches are considered new approach methodologies (NAM) that hold promise for being used by governments, regulators, and businesses in support of more ethical risk assessment approaches (Mondou et al., 2020).

4.4. Conclusions and further directions

This study showed that biotransformation of B[*a*]P can be successfully implemented into TK models to predict the abundances of B[*a*]P metabolites in both the embryo-larval and adult life stages of the fathead minnow. The multi-compartment adult model had slightly better predictive power compared to the embryo-larval one-compartment model. However, both models could be improved through measurements of further model parameters, specifically biotransformation in the embryo-larval developmental stages and bile dynamics in the adult life stage. Additionally, integrating saturation kinetics could increase model applications. Increasing a model's scope and applications is an important development for the use of TK in environmental risk assessment, as it provides a means of estimating impacts of chemical accumulation, as well as reverse dosimetry. This allows for a system to be developed in which chemicals can be prioritized for more extensive *in vivo* testing as suggested by Nichols et al. (2013a). Future work should be focused on parameterizing the current TK models to be extrapolated to other species and biotransformed chemicals.

CRediT authorship contribution statement

Chelsea Grimard: Conceptualization, Methodology, Software, Validation, Formal analysis, Investigation, Data curation, Writing - original draft, Visualization, Project administration. **Annika Mangold-Döring:** Methodology, Software, Validation, Data curation, Writing - review & editing. **Markus Schmitz:** Investigation, Formal analysis, Writing - review & editing. **Hattan Alharbi:** Methodology, Resources. **Paul D. Jones:** Methodology, Resources, Writing - review & editing. **John P. Giesy:** Methodology, Resources, Writing - review & editing. **Markus Hecker:** Conceptualization, Supervision, Funding acquisition, Writing - review & editing. **Markus Brinkmann:** Conceptualization, Methodology, Software, Validation, Formal analysis, Investigation, Resources, Data curation, Writing - review & editing, Supervision, Project administration, Funding acquisition.

Declaration of Competing Interest

The authors declare that they have no known competing financial interests or personal relationships that could have appeared to influence the work reported in this paper.

Acknowledgements

Appendix A. Supplementary data

Supplementary material related to this article can be found, in the online version, at doi:https://doi.org/10.1016/j.aquatox.2020.105616.

References

Ankley, G.T., Villeneuve, D.L., 2006. The fathead minnow in aquatic toxicology: past, present and future. Aquat. Toxicol. 78 (1), 91–102. https://doi.org/10.1016/j.aquatox.2006.01.018.

Arnot, J.A., Gobas, F.A., 2004. A food web bioaccumulation model for organic chemicals in aquatic ecosystems. Environ. Toxicol. Chem. An Int. J. 23 (10), 2343–2355. https://doi.org/10.1897/03-438.

Basu, N., Crump, D., Head, J., Hickey, G., Hogan, N., Maguire, S., et al., 2019. EcoToxChip: a next-generation toxicogenomics tool for chemical prioritization and environmental management. Environ. Toxicol. Chem. 38 (2), 279. https://doi.org/10.1002/etc.4309.

Beach, J.B., Pellizzari, E., Keever, J.T., Ellis, L., 2000. Determination of benzo [a] pyrene and other polycyclic aromatic hydrocarbons (PAHs) at trace levels in human tissues. J. Anal. Toxicol. 24 (8), 670–677. https://doi.org/10.1093/jat/24.8.670.

Booc, F., Thornton, C., Lister, A., MacLatchy, D., Willett, K.L., 2014. Benzo [a] pyrene effects on reproductive endpoints in Fundulus heteroclitus. Toxicol. Sci. 140 (1), 73–82. https://doi.org/10.1093/toxsci/kfu064.

Brinkmann, M., Eichbaum, K., Kammann, U., Hudjetz, S., Cofalla, C., Buchinger, S., et al., 2014. Physiologically-based TK models help identifying the key factors affecting contaminant uptake during flood events. Aquat. Toxicol. 152, 38–46.

Brinkmann, M., Schlechtriem, C., Reininghaus, M., Eichbaum, K., Buchinger, S., Reifferscheid, G., et al., 2016. Cross-species extrapolation of uptake and disposition of neutral organic chemicals in fish using a multispecies physiologically-based TK model framework. Environ. Sci. Technol. 50 (4), 1914–1923. https://doi.org/10.1016/j.aquatox.2014.03.021.

Carrasco-Navarro, V., Jæger, I., Honkanen, J.O., Kukkonen, J.V.K., Carroll, J., Camus, L., 2015. Bioconcentration, biotransformation and elimination of pyrene in the arctic crustacean Gammarus setosus (Amphipoda) at two temperatures. Mar. Environ. Res. 110, 101–109. https://doi.org/10.1016/j.marenvres.2015.08.003.

Costa, J., Ferreira, M., Rey-Salgueiro, L., Reis-Henriques, M.A., 2011. Comparision of the waterborne and dietary routes of exposure on the effects of Benzo (a) pyrene on biotransformation pathways in Nile tilapia (Oreochromis niloticus). Chemosphere 84 (10), 1452–1460. https://doi.org/10.1016/j.chemosphere.2011.04.046.

Costa, J., Reis-Henriques, M.A., Wilson, J.M., Ferreira, M., 2013. P-glycoprotein and CYP1A protein expression patterns in Nile tilapia (Oreochromis niloticus) tissues

after waterborne exposure to benzo (a) pyrene (BaP). Environ. Toxicol. Pharmacol. 36 (2), 611–625. https://doi.org/10.1016/j.etap.2013.05.017.

Crowell, S.R., Amin, S.G., Anderson, K.A., Krishnegowda, G., Sharma, A.K., Soelberg, J. J., Corley, R.A., 2011. Preliminary physiologically based pharmacokinetic models for benzo[a]pyrene and dibenzo[def,p]chrysene in rodents. Toxicol. Appl. Pharmacol. 257 (3), 365–376. https://doi.org/10.1016/j.taap.2011.09.020.

EFSA, 2005. Opinion of the Scientific Panel on Animal Health and Welfare (AHAW) on a request from the Commission related to the aspects of the biology and welfare of animals used for experimental and other scientific purposes. Efsa J. 3 (12) https://doi.org/10.2903/j.efsa.2005.292. N/a.

Embry, M.R., Belanger, S.E., Braunbeck, T.A., Galay-Burgos, M., Halder, M., Hinton, D. E., et al., 2010. The fish embryo toxicity test as an animal alternative method in hazard and risk assessment and scientific research. Aquat. Toxicol. 97 (2), 79–87. https://doi.org/10.1016/j.aquatox.2009.12.008.

European Commission, 2018. EURL ECVAM Fish In Vitro Intrinsic Clearance Database. Retrieved from https://ec.europa.eu/knowledge4policy/node/30101_fr. Date accessed July 14, 2020.

Fay, K.A., Fitzsimmons, P.N., Hoffman, A.D., Nichols, J.W., 2017. Comparison of trout hepatocytes and liver S9 fractions as in vitro models for predicting hepatic clearance in fish. Environ. Toxicol. Chem. 36 (2), 463–471. https://doi.org/10.1002/etc.3572.

Foekema, E.M., Fischer, A., Parron, M.L., Kwadijk, C., de Vries, P., Murk, A.J., 2012. Toxic concentrations in fish early life stages peak at a critical moment. Environ. Toxicol. Chem. 31 (6), 1381–1390. https://doi.org/10.1002/etc.1836.

Franco, M.E., Lavado, R., 2019. Applicability of in vitro methods in evaluating the biotransformation of polycyclic aromatic hydrocarbons (PAHs) in fish: advances and challenges. Sci. Total Environ. 671, 685–695. https://doi.org/10.1016/j.scitotenv.2019.03.394.

Gelboin, H.V., 1980. Benzo[a]pyrene metabolism, activation, and carcinogenesis: role and regulation of mixed-function oxidases and related enzymes. Physiol. Rev. 60 (4), 1107–1166. https://doi.org/10.1152/physrev.1980.60.4.1107.

Gravato, C., Guilhermino, L., 2009. Effects of benzo (a) pyrene on seabass (Dicentrarchus labrax L.): biomarkers, growth and behavior. Hum. Ecol. Risk Assess. 15 (1), 121–137. https://doi.org/10.1080/10807030802615659.

Habig, W.H., Pabst, M.J., Jakoby, W.B., 1974. Glutathione S-transferases the first enzymatic step in mercapturic acid formation. J. Biol. Chem. 249 (22), 7130–7139.

Han, X., Nabb, D.L., Yang, C.H., Snajdr, S.I., Mingoia, R.T., 2009. Liver microsomes and S9 from rainbow trout (Oncorhynchus mykiss): comparison of basal-level enzyme activities with rat and determination of xenobiotic intrinsic clearance in support of bioaccumulation assessment. Environ. Toxicol. Chem. An Int. J. 28 (3), 481–488. https://doi.org/10.1897/08-269.1.

Hawkins, W.E., Walker, W.W., Overstreet, R.M., Lytle, J.S., Lytle, T.F., 1990. Carcinogenic effects of some polycyclic aromatic hydrocarbons on the Japanese medaka and guppy in waterborne exposures. Sci. Total Environ. 94 (1–2), 155–167. https://doi.org/10.1016/0048-9697(90)90370-A.

Hawkins, W.E., Walker, W.W., Lytle, T.F., Lytle, J.S., Overstreet, R.M., 1991. Studies on the Carcinogenic Effects of Benzo (a) Pyrene and 7, 12-dimethylbenz (a) Anthracene on the Sheepshead Minnow (Cyprinodon Variegatus). In *Aquatic Toxicology and Risk Assessment: Fourteenth Volume*. ASTM International. https://doi.org/10.1520/STP23566S.

Heredia-ortiz, R., Bouchard, M., Marie-desvergne, C., Viau, C., Ma.tre, A., 2011. Modeling of the internal kinetics of benzo(a)pyrene and 3-hydroxybenzo(a)pyrene biomarker from rat data. Toxicol. Sci. 122 (2), 275–287. https://doi.org/10.1093/toxsci/kfr135.

Jönsson, M.E., Jenny, M.J., Woodin, B.R., Hahn, M.E., Stegeman, J.J., 2007. Role of AHR2 in the expression of novel cytochrome P450 1 family genes, cell cycle genes, and morphological defects in developing zebra fish exposed to 3, 3′, 4, 4′, 5-penta-chlorobiphenyl or 2, 3, 7, 8-tetrachlorodibenzo-p-dioxin. Toxicol. Sci. 100 (1), 180–193. https://doi.org/10.1093/toxsci/kfm207.

Kais, B., Schiwy, S., Hollert, H., Keiter, S.H., Braunbeck, T., 2017. In vivo EROD assays with the zebrafish (Danio rerio) as rapid screening tools for the detection of dioxin-like activity. Sci. Total Environ. 590, 269–280. https://doi.org/10.1016/j.scitotenv.2017.02.236.

Kennedy, S.W., Jones, S.P., 1994. Simultaneous measurement of cytochrome P4501A catalytic activity and total protein concentration with a fluorescence plate reader. Anal. Biochem. 222 (1), 217–223. https://doi.org/10.1006/abio.1994.1476.

Kennedy, C.J., Tierney, K.B., 2008. Energy intake affects the biotransformation rate, scope for induction, and metabolite profile of benzo [a] pyrene in rainbow trout. Aquat. Toxicol. 90 (3), 172–181. https://doi.org/10.1016/j.aquatox.2008.08.016.

Knöbel, M., Busser, F.J., Rico-Rico, A., Kramer, N.I., Hermens, J.L., Hafner, C., et al., 2012. Predicting adult fish acute lethality with the zebrafish embryo: relevance of test duration, endpoints, compound properties, and exposure concentration analysis. Environ. Sci. Technol. 46 (17), 9690–9700. https://doi.org/10.1021/es301729q.

Lammer, E., Carr, G.J., Wendler, K., Rawlings, J.M., Belanger, S.E., Braunbeck, T., 2009. Is the fish embryo toxicity test (FET) with the zebrafish (Danio rerio) a potential alternative for the fish acute toxicity test? Comp. Biochem. Physiol. Part C Toxicol. Pharmacol. 149 (2), 196–209. https://doi.org/10.1016/j.cbpc.2008.11.006.

Le Fol, V., Brion, F., Hillenweck, A., Perdu, E., Bruel, S., Aït-Aïssa, S., et al., 2017. Comparison of the in vivo biotransformation of two emerging estrogenic contaminants, BP2 and BPS, in zebrafish embryos and adults. Int. J. Mol. Sci. 18 (4), 704. https://doi.org/10.3390/ijms18040704.

Lee, J.W., Kim, Y.H., Yoon, S., Lee, S.K., 2014a. Cytochrome P450 system expression and DNA adduct formation in the liver of Zacco platypus following waterborne Benzo (a) pyrene exposure: implications for biomarker determination. Environ. Toxicol. 29 (9), 1032–1042. https://doi.org/10.1002/tox.21833.

Lee, Y.S., Lee, D.H., Delafoulhouze, M., Otton, S.V., Moore, M.M., Kennedy, C.J., Gobas, F.A., 2014b. In vitro biotransformation rates in fish liver S9: effect of dosing

techniques. Environ. Toxicol. Chem. 33 (8), 1885–1893. https://doi.org/10.1002/etc.2636.

Liu, D., Pan, L., Li, Z., Cai, Y., Miao, J., 2014. Metabolites analysis, metabolic enzyme activities and bioaccumulation in the clam Ruditapes philippinarum exposed to benzo [a] pyrene. Ecotoxicol. Environ. Saf. 107, 251–259. https://doi.org/10.1016/j.ecoenv.2014.06.024.

Lo, J.C., Allard, G.N., Otton, S.V., Campbell, D.A., Gobas, F.A., 2015. Concentration dependence of biotransformation in fish liver S9: optimizing substrate concentrations to estimate hepatic clearance for bioaccumulation assessment. Environ. Toxicol. Chem. 34 (12), 2782–2790. https://doi.org/10.1002/etc.3117.

Long, A., Walker, J.D., 2003. Quantitative structure-activity relationships for predicting metabolism and modeling cytochrome P450 enzyme activities. Environ. Toxicol. Chem. An Int. J. 22 (8), 1894–1899. https://doi.org/10.1897/01-480.

Lu, Y., Ludsin, S.A., Fanslow, D.L., Pothoven, S.A., 2008. Comparison of three microquantity techniques for measuring total lipids in fish. Can. J. Fish. Aquat. Sci. 65 (10), 2233–2241. https://doi.org/10.1139/F08-135.

Lu, D., Harvey, R.G., Blair, I.A., Penning, T.M., 2011. Quantitation of benzo [a] pyrene metabolic profiles in human bronchoalveolar (H358) cells by stable isotope dilution liquid chromatography–atmospheric pressure chemical ionization mass spectrometry. Chem. Res. Toxicol. 24 (11), 1905–1914. https://doi.org/10.1021/tx2002614.

McElroy, A.E., Barron, M.G., Beckvar, N., Driscoll, S.B.K., Meador, J.P., Parkerton, T.F., et al., 2011. A review of the tissue residue approach for organic and organometallic compounds in aquatic organisms. Integr. Environ. Assess. Manag. 7 (1), 50–74. https://doi.org/10.1002/ieam.132.

Miller, M.M., Wasik, S.P., Huang, G.L., Shiu, W.Y., Mackay, D., 1985. Relationships between octanol-water partition coefficient and aqueous solubility. Environ. Sci. Technol. 19 (6), 522–529.

Mondou, M., Hickey, G.M., Rahman, H.T., Maguire, S., Pain, G., Crump, D., et al., 2020. Factors affecting the perception of New Approach Methodologies (NAMs) in the ecotoxicology community. Integr. Environ. Assess. Manag. 16 (2), 269–281. https://doi.org/10.1002/ieam.4244.

Nacalai Tesque Inc, 2017. Cosmosil.Cosmocore Technical Notes. Retrieved from https://www.nacalai.co.jp/global/cosmosil/technicalnote/index.html. Date accessed July 14, 2020.

Nagel, R., 2002. DarT: the embryo test with the zebrafish Danio rerio—a general model in ecotoxicology and toxicology. Altex 19 (Suppl 1), 38–48.

Nichols, J.W., McKim, J.M., Andersen, M.E., Gargas, M.L., Clewell, H.J., Erickson, R.J., 1990. A physiologically based TK model for the uptake and disposition of waterborne organic chemicals in fish. Toxicol. Appl. Pharmacol. 106 (3), 433–447. https://doi.org/10.1016/0041-008X(90)90338-U.

Nichols, J., Schultz, I., Fitzsimmons, P., 2006. In vitro-in vivo extrapolation of quantitative hepatic biotransformation data for fish - I. A review of methods, and strategies for incorporating intrinsic clearance estimates into chemical kinetic models. Aquat. Toxicol. 78 (1), 74–90. https://doi.org/10.1016/j.aquatox.2006.01.017.

Nichols, J.W., Fitzsimmons, P.N., Burkhard, L.P., 2007. In vitro-in vivo extrapolation of quantitative hepatic biotransformation data for fish. II. Modeled effects on chemical bioaccumulation. Environ. Toxicol. Chem. 26 (6), 1304–1319. https://doi.org/10.1897/06-259R.1.

Nichols, J.W., Hoffman, A.D., Fitzsimmons, P.N., 2009. Optimization of an isolated perfused rainbow trout liver model: clearance studies with 7-ethoxycoumarin. Aquat. Toxicol. 95 (3), 182–194. https://doi.org/10.1016/j.aquatox.2009.09.003.

Nichols, J.W., Hoffman, A.D., ter Laak, T.L., Fitzsimmons, P.N., 2013a. Hepatic clearance of 6 polycyclic aromatic hydrocarbons by isolated perfused trout livers: prediction from in vitro clearance by liver S9 fractions. Toxicol. Sci. 136 (2), 359–372. https://doi.org/10.1093/toxsci/kft219.

Nichols, J., Huggett, D., Arnot, J., Fitzsimmons, P., Cowan-Ellsberry, C., 2013b. Toward improved models for predicting bioconcentration of well-metabolized compounds by rainbow trout using measured rates of in vitro intrinsic clearance. Environ. Toxicol. Chem. 32 (7), 1611–1622. https://doi.org/10.1002/etc.2219.

OECD, 2013. Test No. 236: Fish Embryo Acute Toxicity (FET) Test, OECD Guidelines for the Testing of Chemicals, Section 2. OECD Publishing, Paris. https://doi.org/10.1787/9789264203709-en.

OECD, 2018. Test No. 319B: Determination of in Vitro Intrinsic Clearance Using Rainbow Trout Liver S9 Sub-cellular Fraction (RT-S9), OECD Guidelines for the Testing of Chemicals, Section 3. OECD Publishing, Paris. https://doi.org/10.1787/9789264303232-en.

Ortiz-Delgado, J.B., Segner, H., Arellano, J.M., Sarasquete, C., 2007. Histopathological alterations, EROD activity, CYP1A protein and biliary metabolites in gilthead seabream Sparus aurata exposed to benzo (a) pyrene. Histol. Histopathol. (Cell. Molecul. Biol.) 22 (4), 417–432. https://doi.org/10.14670/HH-22.417.

Otte, J.C., Schmidt, A.D., Hollert, H., Braunbeck, T., 2010. Spatio-temporal development of CYP1 activity in early life-stages of zebrafish (Danio rerio). Aquat. Toxicol. 100 (1), 38–50. https://doi.org/10.1016/j.aquatox.2010.07.006.

Peters, L.D., Morse, H.R., Waters, R., Livingstone, D.R., 1997. Responses of hepatic cytochrome P450 1A and formation of DNA-adducts in juveniles of turbot (Scophthalmus maximus L.) exposed to water-borne benzo [a] pyrene. Aquat. Toxicol. 38 (1–3), 67–82. https://doi.org/10.1016/S0166-445X(96)00838-7.

Sandvik, M., Einar Horsberg, T., Utne Skaare, J., Ingebrigtsen, K., 1997. Hepatic CYP1A induction in rainbow trout (Oncorhynchus mykiss) after exposure to benzo [a] pyrene in water. Biomarkers 2 (3), 175–180. https://doi.org/10.1080/135475097231715.

Schiwy, S., Bräunig, J., Alert, H., Hollert, H., Keiter, S.H., 2015. A novel contact assay for testing aryl hydrocarbon receptor (AhR)-mediated toxicity of chemicals and whole sediments in zebrafish (Danio rerio) embryos. Environ. Sci. Pollut. Res. - Int. 22 (21), 16305–16318. https://doi.org/10.1007/s11356-014-3185-0.

Schlenk, D., Celander, M., Gallagher, E.P., George, S., James, M., Kullman, S.W., et al., 2008. Biotransformation in fishes. The toxicology of fishes 153–234. https://doi.org/10.1201/9780203647295.ch4.

Schwerte, T., Voigt, S., Pelster, B., 2005. Epigenetic variations in early cardiovascular performance and hematopoiesis can be explained by maternal and clutch effects in developing zebrafish (Danio rerio). Comp. Biochem. Physiol., Part A Mol. Integr. Physiol. 141 (2), 200–209. https://doi.org/10.1016/j.cbpb.2005.05.042.

Sloman, K.A., McNeil, P.L., 2012. Using physiology and behaviour to understand the responses of fish early life stages to toxicants. J. Fish Biol. 81 (7), 2175–2198.

Stadnicka, J., Schirmer, K., Ashauer, R., 2012. Predicting concentrations of organic chemicals in fish by using TK models. Environ. Sci. Technol. 46 (6), 3273–3280. https://doi.org/10.1021/es2043728.

Stegeman, J.J., Lech, J.J., 1991. Cytochrome P-450 monooxygenase systems in aquatic species: carcinogen metabolism and biomarkers for carcinogen and pollutant exposure. Environ. Health Perspect. 90, 101–109. https://doi.org/10.1289/ehp.90-1519513.

Strobel, A., Burkhardt-Holm, P., Schmid, P., Segner, H., 2015. Benzo (a) pyrene metabolism and EROD and GST biotransformation activity in the liver of red-and white-blooded Antarctic fish. Environ. Sci. Technol. 49 (13), 8022–8032. https://doi.org/10.1021/acs.est.5b00176.

Tang, C., Tan, J., Fan, R., Zhao, B., Tang, C., Ou, W., et al., 2016. Quasi-targeted analysis of hydroxylation-related metabolites of polycyclic aromatic hydrocarbons in human urine by liquid chromatography–mass spectrometry. J. Chromatogr. A 1461, 59–69. https://doi.org/10.1016/j.chroma.2016.07.051.

van den Hurk, P., Gerzel, L.E., Calomiris, P., Haney, D.C., 2017. Phylogenetic signals in detoxification pathways in Cyprinid and Centrarchid species in relation to sensitivity to environmental pollutants. Aquat. Toxicol. 188, 20–25. https://doi.org/10.1016/j.aquatox.2017.04.004.

Wang, L., Camus, A.C., Dong, W., Thornton, C., Willett, K.L., 2010. Expression of CYP1C1 and CYP1A in Fundulus heteroclitus during PAH-induced carcinogenesis. Aquat. Toxicol. 99 (4), 439–447. https://doi.org/10.1016/j.aquatox.2010.06.002.

Yuan, L., Lv, B., Zha, J., Wang, Z., 2017. Benzo [a] pyrene induced p53-mediated cell cycle arrest, DNA repair, and apoptosis pathways in Chinese rare minnow (Gobiocypris rarus). Environ. Toxicol. 32 (3), 979–988. https://doi.org/10.1002/tox.22298.

Zhu, S., Li, L., Thornton, C., Carvalho, P., Avery, B.A., Willett, K.L., 2008. Simultaneous determination of benzo [a] pyrene and eight of its metabolites in Fundulus heteroclitus bile using ultra-performance liquid chromatography with mass spectrometry. J. Chromatogr. B 863 (1), 141–149. https://doi.org/10.1016/j.jchromb.2008.01.018 x.

SUPPLEMENTARY MATERIALS

In vitro-in vivo and cross-life stage extrapolation of uptake and

biotransformation of benzo[a]pyrene in the fathead minnow

(Pimephales promelas)

Chelsea Grimard, Annika Mangold-Döring, Markus Schmitz, Hattan Alharbi, Paul D. Jones,
John P. Giesy, Markus Hecker, Markus Brinkmann

Total page number: 31, including 5 tables and 2 figures

1. Test organism maintenance and housing

Adult fathead minnows used for adult exposures were housed in glass-fiber reinforced plastic tanks (700 L) containing aerated dechlorinated facility water at 22 °C ± 1 °C and a 12 h-light:12 h-dark photoperiod. Fish were fed a diet of frozen *Chironomidae* larvae twice daily (Hikari Sales Inc. Haywards, CA, USA). A second group of adult fathead minnows was used as breeding stock and housed in 20 L aquaria containing facility water within an environmental chamber at a ratio of 2 males: 3 females per tank, at 25 °C ± 1 °C and a 16 h-light:18 h-dark photoperiod. Fish were fed a diet of *Chironomidae* larvae (Hikari Sales Inc.) three times daily. Each breeding tank contained two halves of a PVC pipe to act as a breeding location. Embryos were collected twice daily and placed in glass Petri dishes for immediate use in embryo-larval life stage studies. Water quality parameters (temperature, dissolved oxygen, pH, ammonia) were measured weekly. Temperature (°C), pH, and dissolved oxygen (%) were measured with YSI Professional Plus probe (YSI Incorporated., Yellow Springs, OH, USA), while ammonia was measured using the colorimetric API ammonia test kit (Mars Fishcare, Chalfont, PA, USA).

2. Waterborne B[*a*]P exposures

Waterborne chronic B[*a*]P exposures were conducted to evaluate uptake by and biotransformation of B[*a*]P in the embryo-larval and adult life stages of fathead minnows. Nominal concentrations for both exposures were 1.3, 4.0 or 12.0 µg B[*a*]P/L (benzo[*a*]pyrene, CAS 50-32-8, Sigma-Aldrich, Oakville, ON, CAN) by use of 0.02% DMSO (≥ 99.9% dimethyl sulfoxide, Fisher Scientific Co., Ottawa, ON, CAN) as the solvent carrier, or 0.02% DMSO only as the solvent control. The embryo-larval exposure also included de-chlorinated water from the University of Saskatchewan aquatic toxicology research facility (ATRF) as a water control.

In the first experiment, fathead minnow embryos (<10 hours post-fertilization) were exposed for 32 days following OECD 210: Fish, Early-life stage toxicity test (OECD, 2013).

For the first seven days of exposure, embryos were maintained in a daily 50% static renewal system in glass Petri dishes. Two sets of Petri dishes were maintained with 10 (lipid endpoint: $n=2$ per treatment per sampling point) or 20 (chemical analysis: $n=2$ per treatment per sampling point; biochemical endpoints: $n=3$ per treatment per sampling point) embryos each that were sampled after three and seven days of exposure. One additional set of Petri dishes was maintained with 30 embryos each ($n=5$ per treatment) that were sampled after 14 and 32 days of exposure. At eight days of exposure, larvae from these Petri dishes were transferred to 7-L aquaria containing 5 L of water under flow-through conditions, and the tank volume was replaced four times per day. The temperature was maintained at 25°C ± 1°C. After the 32 days of exposure, three remaining larvae per tank ($n=5$ per treatment) underwent a depuration phase in clean, filtered facility water for an additional seven days. Fish were fed a diet of one or two-day-old *Artemia spp.* nauplii three times daily *ad libitum* starting prior to swim-up, i.e. five days of exposure.

In the second experiment, adult fathead minnow breeding groups consisting of two males and three females were exposed for 21 days (sampling day four and 21 of exposure: $n=5$ per treatment; sampling day seven, 14 and depuration: $n=2$ per treatment) following OECD 229: Fish Short Term Reproduction Assay (OECD, 2012) in 20-L flow-through tanks at approximately three full water replacements per day under a 16 h-light:8 h-dark photoperiod, and 25°C ± 1°C. Tanks were allocated to treatment groups by fecundity (the best 5 performing tanks were randomly assigned to the first replicate of each treatment group, then the next best 5 performing tanks to the second replicate of each treatment group, and so on) to ensure uniform fecundity between treatments at the start of exposure, and the number of eggs produced from each tank was recorded daily for the remainder of the exposure. Post-exposure, remaining tanks underwent a seven-day depuration phase during which they were switched to facility water. Fish were fed *ad libitum* a diet of frozen *Chironomidae* larvae (Hikari Sales Inc.) three times daily during all phases of exposure.

Water quality parameters temperature (°C), dissolved oxygen (%), pH, conductivity (µS/cm), ammonia (mg/L), nitrates (mg/L), nitrites (mg/L), hardness (mg/L), and alkalinity (mg/L) were recorded daily from a manual selection of tanks to ensure each tank was tested once weekly. Temperature, dissolved oxygen, pH, and conductivity were measured using a hand-held digital instrument (YSI Professional Plus, YSI Inc.). Nitrates and nitrites were measured using colorimetric kits, and hardness and alkalinity were measured using titrations kits from LaMotte Co. (Chestertown, MD, USA). Ammonia was measured using the colorimetric API ammonia test kit (Mars Fishcare).

3. Analytical confirmation of B[*a*]P metabolites

The major metabolites 3-hydroxy-benzo[*a*]pyrene (OH-B[*a*]P) and 3-hydroxy-benzo[*a*]pyrene *O*-glucuronide (Gluc-B[*a*]P) were quantified using ultra-high-performance liquid chromatography high-resolution mass spectrometry (UPLC-HRMS) using a modified method described by Beach et al. (2000), Zhu et al. (2008), Lu et al., (2011), and Tang et al. (2016). The quantification method was developed due to the lack of standards available for gluc-B[*a*]P metabolites. Improvements to the standard method, in which total polycyclic aromatic hydrocarbon (PAH) equivalent concentrations were quantified by their quantitative enzymatic conversion into hydroxy-PAHs (OH-PAHs) (Kammann, 2007), were made by being able to obtain measurements that provide information on the relative concentrations of the major metabolite classes.

Metabolite analysis was conducted using a Vanquish UHPLC and Q-Exactive^{TM} HF Quadrupole-Orbitrap^{TM} mass spectrometer (Thermo-Fisher, Waltham, MA, USA). An Acclaim Vanquish 2.2-µm C18 LC column (150 x 2.1 mm) (Thermo-Fisher) using gradient elution with water and acetonitrile (ACN), both containing 0.1% formic acid (pH 2.7) at a flow rate of 0.25 mL/min and column temperature of 30°C was used for LC separation. The run time was 25 minutes in total using a gradient of 25% ACN from 0-3 min, increasing 25% to 100% ACN

from 3-15 minutes, 100% ACN from 15-18 minutes, and re-equilibration for 7 minutes to 25% ACN. The retention time of OH-B[*a*]P was 12.74 and Gluc-B[*a*]P was 8.39

Samples were ionized by negative mode heated electrospray ionization (HESI) followed by a full MS/parallel reaction monitoring (PRM) method which monitored the [M-H]$^-$ parent ion m/z 267.080 for OH-B[*a*]P and both parent and daughter ions for Gluc-B[*a*]P (m/z 443.113 → 267.080). HESI source parameters were as follows: sheath gas flow = 35; aux gas flow = 8; sweep gas flow = 1; aux gas heater = 325°C; spray voltage = 2.7 kV; S-lens RF = 55; capillary temperature = 300°C. The PRM scan settings were: 60,000/30,000 resolution, AGC target = $1x10^6/2x10^5$, max. injection time = 100ms/100ms, full MS scan range of 80-500 *m/z,* PRM isolation window of 2.0 m/z, and normalized collision energy = 30.

Stock solutions of OH-B[*a*]P (CAS 13345-21-6, Toronto Research Chemicals, ON, CAN) were made in HPLC grade methanol/ACN (Fisher Scientific, Waltham, MA, USA). A six-point OH-B[*a*]P calibration curve (0.3, 1, 3, 10, 30, 100 ng/ml, r^2 = 0.9959) was used for semi-quantification of the B[*a*]P metabolites. Concentrations of OH-B[*a*]P were quantified directly with the use of analytical standards and external calibration. To quantify Gluc-B[*a*]P concentrations, a semi-quantification method was used. A representative set of bile samples from B[*a*]P-exposed rainbow trout (*Oncorhynchus mykiss*) were analyzed untreated (25 μL bile, 100 μL purified water), or treated with glucuronidase (25 μL bile, 95 μL purified water, 5 μL 30/60 U/mL glucuronidase; CAS 9001-45-0, Roche, Basel, Switzerland) to convert the glucuronide metabolites into OH-B[*a*]P. The samples were incubated in a shaking incubator (New Brunswick^{TM}, Innova 40$^®$) at 200rpm and 37°C for two hours. Following incubation, the samples were diluted 1:10 in ACN and centrifuged at 1,700×g for 15 minutes. The supernatant was subsequently sampled for quantification of OH-B[*a*]P and Gluc-B[*a*]P following the methods outlined above. These samples provided an instrument relative response factor for semi-quantification. The response factors for glucuronide was calculated as (Eq. S1):

$$Response\ factor = \frac{Peak\ Area\ [OH-BaP]_{treated}}{Peak\ Area\ [Gluc-BaP]_{untreated}} \qquad (S1)$$

The average response factor for Gluc-B[a]P was 7.4. This suggests that for equimolar amounts of OH- and Gluc-B[a]P, the OH-B[a]P response was 7.4 times less sensitive. To obtain an external calibration curve for each metabolite, response factors were used to convert peak areas of OH-B[a]P from the standard curve to Gluc-B[a]P peak areas. Concentrations of each metabolite measured in the extracted whole-body embryo or adult bile samples could then be determined from the peak areas. The recovery of glucuronide was not calculated as no glucuronide standard was available.

4. Measurement of intrinsic clearance

ATP (adenosine triphosphate, CAS 34369-07-8), NADPH (nicotinamide adenine dinucleotide phosphate reduced, CAS 100929-71-3), G6P (glucose-6-phosphate, CAS 54010-71-8), GSH (glutathione reduced, CAS 70-18-8), and UDPGA (uridine 5'-diphosphoglucuronic acid, CAS 63700-19-6) were purchased from Sigma-Aldrich. Two replicates of three pooled fathead minnow livers were used to obtain the S9 fraction. Liver tissue was homogenized in 5 µL homogenization buffer: 1 mg tissue and centrifuged at $9,000 \times g$ for 20 minutes. The supernatant (S9) was sampled for use in the *in vitro* clearance assay, and the protein concentration of the S9 was determined using the BCA (bicinchoninic acid) protein assay. A co-substrate mixture described by Richardson et al. (2016) was generated, with modifications, using ATP (11.1 mM), G6P (5.55 mM), GSH (2.77 mM), NADPH (0.55mM), and UDPGA (0.55mM) reconstituted in phosphate buffer (pH 7.4; 100 mM potassium phosphate, 5 mM magnesium chloride, 5 mM magnesium sulfate), to create a PAPS (3'-phosphoadenosine-5'-phosphosulfate) regenerating system. In a glass cell culture tube, S9 and the co-substrates were combined. The solution was spiked with 250µM B[a]P in ACN to obtain a concentration of 0.5 µM B[a]P and immediately

incubated at 25°C in a shaking incubator (New Brunswick™, Innova 40®). After 0, 20, 40, 60, 80, 100, and 120 minutes, sub-samples of the solution were taken and quenched in ice-cold ACN. Samples were centrifuged at 1700×g for 15 minutes. The supernatant was subsequently analyzed for parent B[a]P concentrations using synchronous fluorescence spectrophotometry in a quartz cuvette (Lumina, Thermo Fisher Scientific, Ottawa, ON, CAN). Parent B[a]P signaled between 400-440 nm and the B[a]P metabolites between 420-480 nm, measured and validated using neat B[a]P and OH-B[a]P standards. The peak area of the B[a]P curve was interpolated from a 6-point standard curve (0.00, 0.03, 0.06, 0.13, 0.25, and 0.50 µM; $r^2 =$ 0.9989) and concentrations were plotted against time. The depletion curve was *log*-transformed, and the first-order depletion rate constant (k) was determined by multiplying the slope of the line by -2.3. Intrinsic clearance ($Cl_{int, in\ vitro}$) was calculated as (Eq. S2):

$$Cl_{int,in\ vitro}(mL\ h^{-1}mg^{-1}) = \frac{k(h^{-1})\cdot volume\ of\ the\ reaction\ (mL)}{reaction\ protein\ concentration\ (mg\ L^{-1})} \qquad (S2)$$

5. EROD assay

EROD (7-ethoxyresorufin-*O*-deethylase) activity was measured in triplicates following the protocol previously described by Kennedy & Jones (1994), with modifications. BSA (bovine serum albumin, CAS 9048-46-8), EDTA (Ethylenediaminetetraacetic acid, CAS 6381-92-6), DTT (DL-dithiothreitol, CAS 3483-12-3), fluorescamine (CAS 38183-12-9), HEPES (CAS 7365-45-9), KCL (potassium chloride, CAS 7447-40-7), NADPH (nicotinamide adenine dinucleotide phosphate reduced, CAS 100929-71-3), resorufin (CAS 653-78-9), sucrose (CAS 57-50-1), and Tris-HCl (Trizma®Base, CAS 77-86-1) were purchased from Sigma-Aldrich (Oakville, ON, CAN). Ethoxyresorufin (CAS 5725-91-7) was purchased from Fisher Scientific Co. (Ottawa, ON, CAN). The post-mitochondrial supernatant fraction was generated from the whole-body larvae and adult liver samples following a modified protocol of what is described by OECD 319B (OECD, 2018). Tissue was homogenized in homogenization buffer (150 mM

Tris-HCl, 150 mM KCl, 2 mM EDTA, 1 mM DTT, 250 mM sucrose) at a ratio of 20 µL buffer: 1 mg tissue then centrifuged at 10,000 × g. Six-point resorufin (0, 1.9, 3.8, 7.5, 15, 60 µM) and protein (0, 0.006, 0.012, 0.024, 0.036, 0.48 µM) standard curves were produced by adding HEPES buffer (0.05 M, pH 7.8), BSA (2 mg/mL in HEPES), and resorufin (1.9 µM in HEPES) to six sets of triplicate wells of a 96 well plate. In separate wells, in darkness for 10 minutes. Following incubation, NADPH (0.3 mM in HEPES, 10 µL) was added to all wells, except the sample blanks, to initiate the reaction and the plate was incubated at 25 °C in darkness for 30 minutes. The reaction was stopped by the addition of fluorescamine in ACN (600 µg/mL; 60 µL) to all used wells and the plate was incubated at room temperature in darkness for 15 minutes. Fluorescence of resorufin was read at 570 nm excitation/ 630 nm emission and proteins at 365 nm excitation/ 480 nm emission using a multi-well plate reader (POLARstar Optima, BMG Labtech, Ortenberg, Germany).

6. GST assay

GST (glutathione-*S*-transferase) activity was measured in triplicates following the protocol described by Habig et al. (1974), adapted to microplates. The reagents CDNB (1-Chloro-2,4-dinitrobenzene, CAS 97-00-7), GSH (glutathione reduced, CAS 70-18-8), and potassium phosphate were purchased from Sigma-Aldrich. The post-mitochondrial supernatant fraction was produced as described for the EROD assay. Phosphate buffer (0.1 M, pH 6.5, 275 µL or 250 µL) was added to all wells for sample blanks and active wells respectively, followed by the post-mitochondrial supernatant fraction (20 µL) and CDNB (25 mM in ethanol; 10 µL). To initiate the reaction, GSH (11.4 mM in phosphate buffer; 25 µL) was added to active wells. A kinetic reading of absorbance was immediately started at 340 nm and 25°C for 10 minutes using a multi-well plate reader (POLARstar Optima, BMG Labtech). The concentration of CDNB was calculated using the Lambert-beer law. To calculate GST activity (nmol CDNB/mg protein/min), the molar extinction coefficient of 9.6 1/(mM cm) was used. The protein

concentration of the post-mitochondrial supernatant fraction was measured using the BCA (bicinchoninic acid) protein assay kit (SKU BCA1; Sigma-Aldrich).

7. Lipid analysis

Total whole-body lipid content in both life stages was quantified using a modification of the microcolorimetric sulfophosphovanillin (SPV) described by Lu et al. (2008). Sulphuric acid (CAS 7664-93-9) and phosphoric acid (CAS 7664-38-2) were purchased from Thermo Fisher Scientific, and vanillin (CAS 48-53-8) was purchased from Sigma-Aldrich. Lipids were extracted in triplicates using whole-body fish (embryo-larval, 10-50 mg wet weight; adult, 10-50 mg homogenized sub-sample) homogenized in a 2:1 mixture (v/v) of chloroform and methanol followed by saline (200µl) for lipid purification. In instances in which sample weight exceeded 50 mg, extra chloroform:methanol (200 µL) was added to ensure complete homogenization of the sample and appropriate lipid concentrations. Lipid extracts (200 µL) were evaporated in 5-mL glass culture tubes using a dry bath heater, and lipids subsequentially quantified by the addition of sulphuric acid (62.5 µL) and SPV reagent (1.25 mL of a solution containing 0.75 g vanillin in 0.125 L deionized water and 0.5 L phosphoric acid). Absorbance was measured at 525nm from a 96-well plate using a multi-well plate reader (POLARstar Optima, BMG Labtech, Ortenberg, Germany). A 6-point standard curve (0.00, 0.16, 0.31, 0.63, 1.25, 5.00 mg/mL; $r^2 = 0.9971$) was developed from a serial dilution of cod liver oil (CAS 8001-69-2, Sigma Aldrich) in 2:1 (v/v) chloroform:methanol and used to determine total lipid content of the samples.

8. One-compartment embryo-larval life stage model

The one-compartment bioaccumulation model described by Arnot and Gobas (2004) was adapted to predict the abundance of parent B[*a*]P and B[*a*]P metabolites in the ELS (embryo-larval stage) of fathead minnow exposed aqueously to B[*a*]P (Supplemental Table S2). To adapt

the model to account for biotransformation of B[a]P, a whole-body biotransformation rate constant (k_{met}) was implemented into the model. The whole-body biotransformation rate constant was calculated using an Excel spreadsheet provided by Nichols, Fitzsimmons, & Burkhard (2007) which used the parameters cardiac output, liver blood flow, and hepatic clearance (Supplemental Table S1). The model was implemented using Python 3.5® (Python Software Foundation, Wilmington, DE, USA) in Jupyter Notebook® (Project Jupyter, U.S. Patent & Trademark Office, Alexandria, VA, USA). A series of matrices were used for the parameters wet weight (w_w), whole-body lipid content (lipid) and the whole body chemical transformation rate constant (k_met) to describe the time function of parameters, i.e. the relationship between the parameter value and life stage (i.e, 0, 3, 7, 14, 32 or 39 days post fertilization (dpf)). A simulated exposure was run at the three measured average exposure concentrations, 0.16, 0.85 and 4.55 µg B[a]P/L for 32 days, 1000 iteration steps per day. Using the model the accumulation of B[a]P and B[a]P metabolites were predicted in the whole-body fathead minnow larvae.

Supplemental Table S1. Spreadsheet inputs and parameters for the embryo-larval life stage of fathead minnow (*Pimephales promelas*) to calculate whole-body biotransformation rate. The table is based on Nichols, Fitzsimmons, & Burkhard (2007).

Symbol	Units	Description	Value		
			Egg stage (0-3 dpf)	Yolk stage (3-7 dpf)	Free feeding stage (7-32 dpf)
Rate	h^{-1}	Depletion rate constant[a]	– Adult value assumed (Supplemental Table S3) –		
Bwg	g	Fish wet weight	0.00122	0.00079	0.00348
log K_{ow}	-	Octanol-water partitioning coefficient	6.19		
C_{S9}	mg mL^{-1}	S9 protein concentration	– Adult value assumed (Supplemental Table S3) –		
L_{S9}	mg g liver^{-1}	Total liver S9 protein content	– Adult value assumed (Supplemental Table S3) –		
L_{FBW}	g liver g wet weight^{-1}	Fractional liver weight	– Adult value assumed (Supplemental Table S3) –		
V_{LWB}	-	Fractional whole-body lipid content	0.0182	0.017	0.029
Q_C	L d^{-1} kg^{-1}	Cardiac output	34.980	110.868	39.528
Q_{HFRAC}	-	Liver blood flow as a fraction of cardiac output	– Adult value assumed (Supplemental Table S3) –		
V_{WBL}	-	Fractional blood water content	– Adult value assumed (Supplemental Table S3) –		
f_u	-	Binding correction term	1.0 (assumed)		
$CL_{int,\ in\ vitro}$	mL h^{-1} mg S9 protein^{-1}	*In vitro* intrinsic clearance	– Equation S3 –		
$CL_{int,\ in\ vivo}$	L d^{-1} kg^{-1}	*In vivo* intrinsic clearance	– Equation S4 –		
Q_H	L d^{-1} kg^{-1}	Liver blood flow	– Equation S5–		
Cl_H	L d^{-1} kg^{-1}	Hepatic clearance	– Equation S6 –		
P_{bw}	-	Blood:water partitioning coefficient	– Equation S7 –		

BCF$_P$	L kg^{-1}	Partitioning based BCF	– Equation S6 –
V$_{D,BL}$	L kg^{-1}	Volume of distribution to blood plasma	– Equation S7 –
k$_{met}$	d^{-1}	Whole-body biotransformation rate	– Equation S8 –

[a]*derived from methods described in OECD 319B: Determination of in vitro clearance using rainbow trout liver S9 sub-cellular fraction (RT-S9) (OECD, 2018)*

Spreadsheet equations for calculation of k$_{met}$ (Nichols et al., 2007)

In vitro intrinsic clearance

$$Cl_{int,in\ vitro} = \frac{rate}{C_{S9}} \ ; \text{(mL h}^{-1}\text{ mg S9 protein}^{-1}\text{)} \tag{Eq. S3}$$

In vivo intrinsic clearance

$$CL_{int,in\ vivo} = CL_{in\ vitro,int} \cdot L_{S9} \cdot L_{FBW} \cdot 24h \ ; \text{(L d}^{-1}\text{ kg}^{-1}\text{)} \tag{Eq. S4}$$

Liver blood flow

$$Q_H = Q_C \cdot Q_{HFRAC} \ ; \text{(L d}^{-1}\text{ kg}^{-1}\text{)} \tag{Eq. S5}$$

Hepatic clearance

$$CL_H = \frac{Q_H \cdot f_u \cdot CL_{in\ vivo,int}}{Q_H + f_u \cdot CL_{in\ vivo,int}} \ ; \text{(L d}^{-1}\text{ kg}^{-1}\text{)} \tag{Eq. S6}$$

Blood:water partition coefficient

$$P_{bw} = 10^{0.73 \cdot log\ K_{ow}} \cdot 0.16 + V_{WBL} \ ; \text{(unitless)} \tag{Eq. S7}$$

Partitioning based bioaccumulation factor

$$BCF_P = V_{LWB} \cdot 10^{log\ k_{ow}} \ ; \text{(L kg}^{-1}\text{)} \tag{Eq. S8}$$

Volume of distribution to blood plasma

$$V_{D,BL} = \frac{BCF_P}{P_{BW}} \ ; \text{(L kg}^{-1}\text{)} \tag{Eq. S9}$$

Whole body biotransformation rate

$$k_{met} = \frac{CL_H}{V_{D,BL}} \ ; \text{(d}^{-1}\text{)} \tag{Eq. S10}$$

Supplemental Table S2. Model inputs and parameters of the one-compartment model for the embryo-larval life stage of fathead minnow (*Pimephales promelas*). The table is based on Arnot and Gobas (2004). The compartment is assumed to have a specific gravity of 1.0 (i.e. the units L and kg can be substitute for another).

Symbol	Units	Description	Value		
			Egg stage (0-3 dpf)	Yolk stage (3-7 dpf)	Free feeding stage (7-32 dpf)
w_w	kg (L)	Body wet weight (volume of the whole body)	– Model input –		
K_{ow}	-	Octanol-water partitioning coefficient	– Model input –		
S	%	Dissolved oxygen saturation	– Model input –		
T	°C	Water temperature	– Model input –		
C_w	µg L^{-1}	Chemical concentration in water	– Model input –		
f_lipid	%	Total lipid content (fraction of body weight)	– Model input –		
lipid	kg	Total lipid content	– Equation S11 –		
β	-	Sorption capacity constant	0.05[*]	0.05[*]	0.05[*]
d_w	kg	Body dry weight	0.28 w_w		
f_NLOM	-	Fraction of non-lipid organic matter	– Equation S12 –		
f_water	-	Water content	– Equation S13 –		
K_{bw}	-	Fish – water partition coefficient	– Equation S14 –		
C_{ox}	mg O$_2$ L^{-1}	Dissolved oxygen concentration in water	– Equation S15 –		
G_v	L d^{-1}	Gill ventilation rate	– Equation S16 –		
E_w	-	Gill chemical uptake efficiency	– Equation S17 –		

k_{in}	L kg^{-1} d^{-1}	Aqueous uptake clearance rate constant	– Equation S18 –
k_{out}	kg kg^{-1} d^{-1}	Gill elimination rate constant	– Equation S19 –
k_G	d^{-1}	Growth dilution rate constant	– Equation S20 –
k_{met}	d^{-1}	Whole-body biotransformation rate	– Equation S10 –
C_{int}	µg g^{-1}	Chemical internal concentration	– Equation S21 –
C_{met}	µg g^{-1}	Metabolite internal concentration	– Equation S22 –

[*] Value is different than what is reported by Arnot & Gobas (2004). Value obtained from DeBruyn & Gobas (2007) as suggested by Stadnicka et al. (2012).

Embryo-larval stage one-compartment model equations (from Arnot and Gobas, 2004)

Total lipid content

$$lipid = w\_w \cdot f\_lipid \; ; \text{(kg)} \qquad \textbf{(Eq. S11)}$$

Fraction of non-lipid organic matter

$$f\_NLOM = \frac{d\_w - lipid}{w\_w} \; ; \text{(unitless)} \qquad \textbf{(Eq. S12)}$$

Water fraction in fish

$$f\_water = \frac{w\_w - d\_w}{w\_w} \; ; \text{(unitless)} \qquad \textbf{(Eq. S13)}$$

Fish – water partition coefficient

$$k_{bw} = f\_lipid \cdot K_{ow} + f\_NLOM \cdot \beta \cdot K_{OW} + f\_water \; ; \text{(unitless)} \qquad \textbf{(Eq. S14)}$$

Dissolved oxygen concentration

$$C_{ox} = (-0.24 \cdot T + 14.04) \cdot \frac{S}{100} \; ; \text{(mg O}_2\text{ L}^{-1}) \qquad \textbf{(Eq. S15)}$$

Gill ventilation rate

$$G_v = 1400 \cdot \frac{w\_w^{0.65}}{C_{ox}} \; ; \text{(L d}^{-1}) \qquad \textbf{(Eq. S16)}$$

Gill chemical uptake efficiency

$$E_w = \frac{1}{1.85 + \frac{155}{K_{ow}}} \; ; \text{(unitless)} \qquad \textbf{(Eq. S17)}$$

Aqueous uptake clearance rate constant

$$k_{in} = \frac{E_w \cdot G_v}{w\_w} \; ; \text{(L kg}^{-1}\text{ d}^{-1}) \qquad \textbf{(Eq. S18)}$$

Gill elimination rate constant

$$k_{out} = \frac{k_{in}}{k_{bw}} \; ; \text{(kg kg}^{-1}\text{ d}^{-1}) \qquad \textbf{(Eq. S19)}$$

Growth dilution rate constant

$$k_G = 0.005 \cdot w\_w^{-0.2} \; ; \text{(d}^{-1}\text{ for temperatures around 10°C)}$$

$$k_G = 0.00251 \cdot w\_w^{-0.2} \; ; \text{(d}^{-1}\text{ for temperatures around 25°C)} \qquad \textbf{(Eq. S20)}$$

Chemical internal concentration

$$\frac{dC_{int}(t)}{dt} = \frac{k_{in}}{1000} \cdot C_w(t) - (k_{out} + K_G) \cdot C_{int}(t) \; ; (\mu g \; g^{-1} \; d^{-1}) \qquad \textbf{(Eq. S21)}$$

Additional model equation (implementation of whole-body chemical biotransformation)

Metabolite internal concentration

$$\frac{dC_{met}(t)}{dt} = k_{met} \cdot C_{int}(t) \; ; (\mu g \; g^{-1} \; d^{-1}) \qquad \textbf{(Eq. S22)}$$

9. Adult multi-compartment physiologically based toxicokinetic (PBTK) model

A multi-compartment PBTK (physiologically based toxicokinetic) model was adapted to predict the abundance of parent B[*a*]P in the tissues and B[*a*]P metabolites in the bile of adult life stage fathead minnow (Stadnicka, Schirmer, & Ashauer, 2012; Brinkmann et al., 2016). The model was adapted to integrate biotransformation of parent B[*a*]P by incorporating an *in vivo* intrinsic clearance parameter calculated using an Excel spreadsheet provided by Nichols, Fitzsimmons, & Burkhard (2007) (Supplemental Table S3). The *in vivo* intrinsic clearance parameter was used to calculate hepatic clearance, using the well-stirred model of hepatic clearance, which was further used to calculate hepatic biotransformation. A bile compartment was implemented into the existing model structure, by combining hepatic biotransformation with bile volume and bile flow, which simulated the mass flux of B[*a*]P metabolites exiting the liver and entering the bile (Supplemental Table S4). The model was implemented using Python 3.5® (Python Software Foundation, Wilmington, DE, USA) in Jupyter Notebook® (Project Jupyter, U.S. Patent & Trademark Office, Alexandria, VA, USA). A simulation was run using input data from 157 adult fathead minnows. The physiological parameters wet weight and bile volume were described for each individual fish along with the exposure parameters, chemical concentration in the water, exposure time, simulation time, temperature and dissolved oxygen. Simulated exposures were run for either 96, 168, 336, or 504 hours, with 5000 iteration steps per hour, at the measured concentrations of either 0.03, 0.08 or 1.34 µg B[*a*]P/L. The model predicted the accumulation of parent B[*a*]P in the whole body, as well as the liver, fat, richly perfused tissues, and poorly perfused tissues, and the accumulation of B[*a*]P metabolites in the bile of adult fathead minnows. Outputs of bile metabolites were multiplied by 0.6 (Equation 40) to represent specific fractions of hydroxy B[*a*]P and the associated glucuronide, which was determined to between 58-66% of total B[*a*]P metabolites produced in adult fish (Zhu et al., 2008). It should also be noted that the kidney was not included in the model as physiological values for the kidney parameters were not available for fathead minnow. However, the model

equations for the kidney are included in the event that the values become available or the model is used for another species.

Supplemental Table S3. Spreadsheet inputs and parameters for adult fathead minnow (*Pimephales promelas*) to calculate hepatic clearance. The table is based on Nichols et al. (2007).

Symbol	Units	Description	Value
Rate	h^{-1}	Depletion rate constant[a]	0.78
C_{S9}	$mg\ mL^{-1}$	S9 protein concentration	1
L_{S9}	$mg\ g\ liver^{-1}$	Total liver S9 protein content	71
L_{FBW}	$g\ liver\ g\ wet\ weight^{-1}$	Fractional liver weight	0.018[b]
Q_C	$L\ d^{-1}\ kg^{-1}$	Cardiac output	924.582[b]
Q_{HFRAC}	-	Liver blood flow as a fraction of cardiac output	0.286[b]
f_u	-	Binding correction term	1.0 (assumed)
$CL_{int,\ in\ vitro}$	$mL\ h^{-1}\ mg\ S9\ protein^{-1}$	*In vitro* intrinsic clearance	– Equation S3 –
$CL_{int,\ in\ vivo}$	$L\ d^{-1}\ kg^{-1}$	*In vivo* intrinsic clearance	– Equation S4 –
Q_H	$L\ d^{-1}\ kg^{-1}$	Liver blood flow	– Equation S5 –
Cl_H	$L\ d^{-1}\ kg^{-1}$	Hepatic clearance	– Equation S6 –

[a]*Derived from methods described in OECD 319B: Determination of in vitro clearance using rainbow trout liver S9 sub-cellular fraction (RT-S9) (OECD, 2018)*
[b]*Data taken from adult fathead minnow multi-compartment PBTK model (Supplemental Table S4)*

Supplemental Table S4. Model inputs and parameters of the multi-compartment PBTK model for adult fathead minnow (*Pimephales promelas*). The table is based on Stadnicka et al. (2012). Compartment volumes were expressed relative to the total body volume, while all compartments were assumed to have a specific gravity of 1.0 (i.e., the units L and kg can be substitute for another).

Symbol	Units	Description	Value
w_w	kg (L)	Body wet weight (volume of the whole body)	– Model input –
$\log K_{ow}$	-	Octanol-water partitioning coefficient	– Model input –
C_w	$\mu g\ L^{-1}$	Chemical concentration in inspired water	– Model input –
T	°C	Water temperature	– Model input –
C_{ox}	$mg\ L^{-1}$	Dissolved oxygen concentration in inspired water	– Model input –
lipid	-	Total lipid content (fraction of body weight)	– Model input –
K	-	Constant in equation S23, for T>10°C	$3.05\ 10^{-4}$ [a]
n	-	Constant in equation S23, for T>10°C	1.855[a]
m	-	Constant in equation S23, for T>10°C	-0.138[a]
α_b	-	Lipid content of blood tissue (fraction of wet weight)	0.019[a]
α_f	-	Lipid content of fat tissue (fraction of wet weight)	1.010[a]
α_k	-	Lipid content of kidney tissue (fraction of wet weight)	–
α_l	-	Lipid content of liver tissue (fraction of wet weight)	0.074[a]
α_m	-	Lipid content of muscle tissue (fraction of wet weight)	0.025[a]
γ_b	-	Water content of blood tissue (fraction of wet weight)	0.876[a]
γ_f	-	Water content of fat tissue (fraction of wet weight)	0.016[a]
γ_k	-	Water content of kidney tissue (fraction of wet weight)	–

γ_l	-	Water content of liver tissue (fraction of wet weight)	0.766[a]
γ_m	-	Water content of muscle tissue (fraction of wet weight)	0.806[a]
$lipid_l$	-	Lipid content of lean tissue (fraction of wet weight)	– Equation S23 –
V_f	L	Volume of the fat compartment	– Equation S24 –
V_k	L	Volume of the kidney compartment	–
V_l	L	Volume of the liver compartment	0.018 w_w
V_m	L	Volume of the poorly perfused compartment	– Equation S25 –
V_r	L	Volume of the richly perfused compartment	0.072 w_w
V_{bile}	L	Volume of bile compartment	– Model input –
Q_c	L h^{-1}	Cardiac output	– Equation S26 –
Q_f	L h^{-1}	Blood flow to the fat compartment	0.010 Q_c
Q_k	L h^{-1}	Blood flow to the kidney compartment	–
Q_l	L h^{-1}	Blood flow to the liver compartment	0.024 Q_c
Q_m	L h^{-1}	Blood flow to the poorly perfused compartment	0.440 Q_c
Q_r	L h^{-1}	Blood flow to the richly perfused compartment	0.526 Q_c
Q_{bile}	L h^{-1}	Bile flow	0.5 V_{bile}
VO_2	mg h^{-1}	Oxygen consumption rate normalized to 1 kg body weight	– Equation S27 –
Q_w	L h^{-1}	Effective respiratory volume	– Equation S28 –
P_{bw}	-	Blood:water partitioning coefficient	– Equation S29 –
P_l, P_f, P_m	-	Liver/fat/muscle:blood partitioning coefficient	– Equation S30 –
P_k	-	Kidney:blood partitioning coefficient	–
P_r	-	Richly perfused tissue:blood partitioning coefficient	– P_l –

A_i	μg	Chemical amount in fat, poorly and richly perfused tissues	– Equation S32 –
A_l	μg	Chemical amount in the liver compartment	– Equation S33 –
$A_{l\_transform}$	μg	Hepatic biotransformation	– Equation S38 –
A_k	μg	Chemical amount in the kidney compartment	–
A_{bile}	μg	Chemical amount in bile compartment	– Equation S39 –
$CL_{int,\ in\ vivo}$	L d^{-1} kg^{-1}	*In vivo* intrinsic clearance	– Equation S4 –
Cl_H	L d^{-1} kg^{-1}	Hepatic clearance	– Equation S6 –
C_{int}	μg g^{-1}	Internal concentration in the whole fish	– Equation S35 –
C_{art}	μg L^{-1}	Chemical concentration in arterial blood	– Equation S36 –
C_{ven}	μg L^{-1}	Chemical concentration in venous blood	– Equation S37 –
C_{bile}	μg L^{-1}	Metabolite concentration in bile	– Equation S40 –

^aData taken from from Stadnicka et al. (2012)

Multi-compartment PBTK model equations (from Stadnicka et al. 2012)

Volume of the lean tissue compartment - cyprinids

$$lipid_l = \frac{V_l \cdot \alpha_l + V_r \cdot \alpha_r + V_m \cdot \alpha_m}{V_l + V_r + V_m} \; ; \text{(unitless)} \qquad \textbf{(Eq. S23)}$$

Volume of the fat compartment

$$V_f = w\_w \cdot \frac{lipid - lipid_l}{\alpha_f - lipid_l} \; ; \text{(L)} \qquad \textbf{(Eq. S24)}$$

Volume of the poorly perfused compartment - cyprinids

$$V_m = w\_w - (V_l + V_r + V_f) \; ; \text{(L)} \qquad \textbf{(Eq. S25)}$$

Cardiac output

$$Q_c = (0.23 \cdot T - 0.78) \cdot \left(\frac{1000 \cdot w\_w}{500}\right)^{-0.1} \cdot w\_w^{0.75} \; ; \text{(L h}^{-1}\text{)} \qquad \textbf{(Eq. S26)}$$

Oxygen consumption rate

$$VO_2 = K \cdot (32 + T \cdot \tfrac{9}{5})^n \cdot \left(\frac{w\_w}{0.4536}\right)^m \cdot \frac{10000}{24} \; ; \text{(mg h}^{-1}\text{)} \qquad \textbf{(Eq. S27)}$$

Effective respiratory volume

$$Q_w = \frac{VO_2}{C_{ox} - 0.2 \cdot C_{ox}} \cdot w\_w^{0.75} \; ; \text{(L h}^{-1}\text{)} \qquad \textbf{(Eq. S28)}$$

Blood:water partitioning coefficient

$$P_{bw} = 10^{0.72 \cdot \log Kow + 1.04 \cdot log(\alpha_b) + 0.86} + \gamma_b \; ; \text{(unitless)} \qquad \textbf{(Eq. S29)}$$

Liver/fat/muscle:blood partitioning coefficient

$$P_{l,f,m} = \frac{10^{0.72 \cdot \log Kow + 1.04 \cdot log(\alpha_{l,f,m}) + 0.86 + \gamma_{l,f,m}}}{P_{bw}} \; ; \text{(unitless)} \qquad \textbf{(Eq. S30)}$$

Kidney:blood partitioning coefficient

$$P_k = \frac{10^{0.72 \cdot \log Kow + 1.04 \cdot log(\alpha_k) + 0.86 + \gamma_k}}{P_{bw}} \; ; \text{(unitless)} \qquad \textbf{(Eq. S31)}$$

Chemical amount in fat, poorly and richly perfused tissues

$$\frac{dA_i(t)}{dt} = Q_i \cdot \left(C_{art}(t) - \frac{A_i(t)}{V_i \cdot P_i}\right) ; (\mu g\ h^{-1}) \qquad \textbf{(Eq. S32)}$$

Chemical amount in the liver compartment

$$\frac{dA_l(t)}{dt} = Q_r \cdot \frac{A_r(t)}{V_r \cdot P_r} + Q_l \cdot C_{art}(t) - (Q_r + Q_l) \cdot \frac{A_l(t)}{V_l \cdot P_l} - A_l\_transform(t) ; (\mu g\ h^{-1})\ \textbf{(Eq. S33)}$$

Chemical amount in the kidney compartment

$$\frac{dA_k(t)}{dt} = 0.6 \cdot Q_m \cdot \frac{A_m(t)}{V_m \cdot P_m} + Q_k \cdot C_{art}(t) - (0.6 \cdot Q_m + Q_k) \cdot \frac{A_k(t)}{V_k \cdot P_k} ; (\mu g\ h^{-1})\ \textbf{(Eq. S34)}$$

Internal chemical concentration in the whole fish - cyprinids

$$C_{int}(t) = \frac{A_f(t) + A_m(t) + A_r(t) + A_l(t)}{1000 \cdot w\_w} ; (\mu g\ g^{-1}) \qquad \textbf{(Eq. S35)}$$

Chemical concentration in arterial blood

$$C_{art}(t) = \min(Q_w, Q_c \cdot P_{bw}) \cdot C_w - \frac{C_{ven}(t)}{P_{bw}} \cdot \frac{1}{Q_c} + C_{ven}(t) ; (\mu g\ L^{-1}) \qquad \textbf{(Eq. S36)}$$

Chemical concentration in venous blood - cyprinids

$$C_{ven}(t) = \left(Q_f \cdot \frac{A_f(t)}{V_f \cdot P_f} + Q_m \cdot \frac{A_m(t)}{V_m \cdot P_m} + (Q_r + Q_l) \cdot \frac{A_l(t)}{V_l \cdot P_l}\right) \cdot \frac{1}{Q_c} ; (\mu g\ L^{-1}) \qquad \textbf{(Eq. S37)}$$

Additional model equations (implementation of chemical biotransformation and bile compartment)

Hepatic biotransformation

$$\frac{dA_l\_transform(t)}{dt} = Cl_H \cdot \frac{A_l}{V_l \cdot P_l} ; (\mu g\ h^{-1}) \qquad \textbf{(Eq. 38)}$$

Chemical amount in the bile

$$A_{bile} = A_{bile} - A_{bile} \cdot \frac{Q_{bile}}{V_{bile}} ; (\mu g\ h^{-1}) \qquad \textbf{(Eq.39)}$$

Metabolite concentration in bile

$$C_{bile}(t) = \frac{A_{bile}}{V_{bile}} \cdot 0.60 ; (\mu g\ L^{-1}) \qquad \textbf{(Eq.40)}$$

10. Sensitivity analyses

Sensitivity analyses were run to assess the influence of changes in several model parameters on model outputs. For the one-compartment ELS model, the parameters wet weight, lipid content, and k_{MET}, were increased and decreased two-fold, respectively. The parameters *in vivo* intrinsic clearance, bile volume, and bile flow were analyzed for the adult multi-compartment PBTK model. *In vivo* intrinsic clearance was changed three-fold and bile volume was changed two-fold in each direction. Bile flow was decreased two-fold and increased by half a factor. Only one parameter was changed at a time by two steps in each direction, while the other parameters remained at their default value.

The sensitivity analysis for the one-compartment ELS model displayed that k_{MET} had the largest influence on model predictions (Supplemental Figure S2C). Model predictions were sensitive to wet weight at low values and became less sensitive as values increased. The model was insensitive to changes in lipid content. All three parameters analyzed for the adult multi-compartment PBTK model exhibited sensitivity at low values and became progressively insensitive to changes as values increased (Supplemental Figure S2D,E,F).
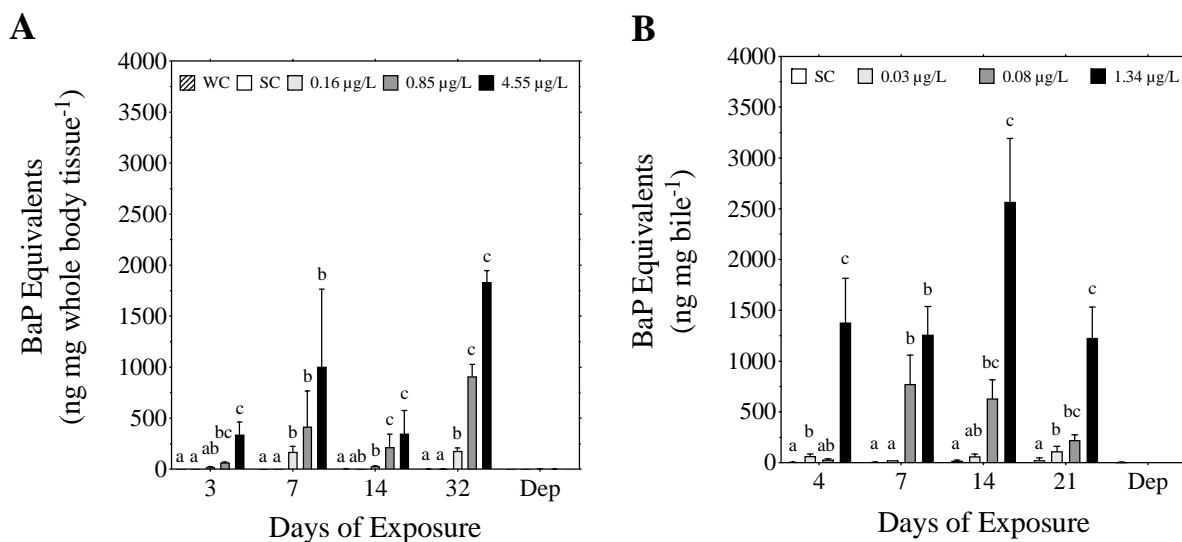
11. Results

Table S5. Time-resolved aqueous B[a]P concentrations for the embryo-larval and adult fathead minnow exposures

Embryo-larval exposure sampling times (day)	Low concentration (µg B[a]P/L)	Medium concentration (µg B[a]P/L)	High concentration (µg B[a]P/L)
1	0.03	0.30	2.00
15	0.12	0.62	3.54
30	0.32	1.64	8.11

Adult exposure sampling times (day)	Low concentration (µg B[a]P/L)	Medium concentration (µg B[a]P/L)	High concentration (µg B[a]P/L)
2	0.04	0.07	1.18
11	0.02	0.09	0.73
20	0.03	0.11	2.1

Figure S1. Abundance of B[*a*]P equivalents (ng mg whole body tissue^{-1} or ng mg bile^{-1}) in whole body embryo-larval (A) or the bile of adult (B) fathead minnows after three, seven, 14 and 32 or four, seven, 14 and 21 days of exposure to increasing concentrations of B[*a*]P as well as water control (WC) and solvent control (SC), respectively. B[*a*]P equivalents were calculated as mass concentrations that are independent of differences in molecular weight of the parent B[*a*]P and the metabolites from measured concentrations of 3-OH-B[*a*]P and associated glucuronide (metabolite specific data provided in the main document Figure 1). Data is expressed as mean ± S.E.M. Different letters denote a significant difference in B[*a*]P equivalents among treatment groups within each respective time point (2-way ANOVA with Tukey's HSD, $\alpha = 0.05$).
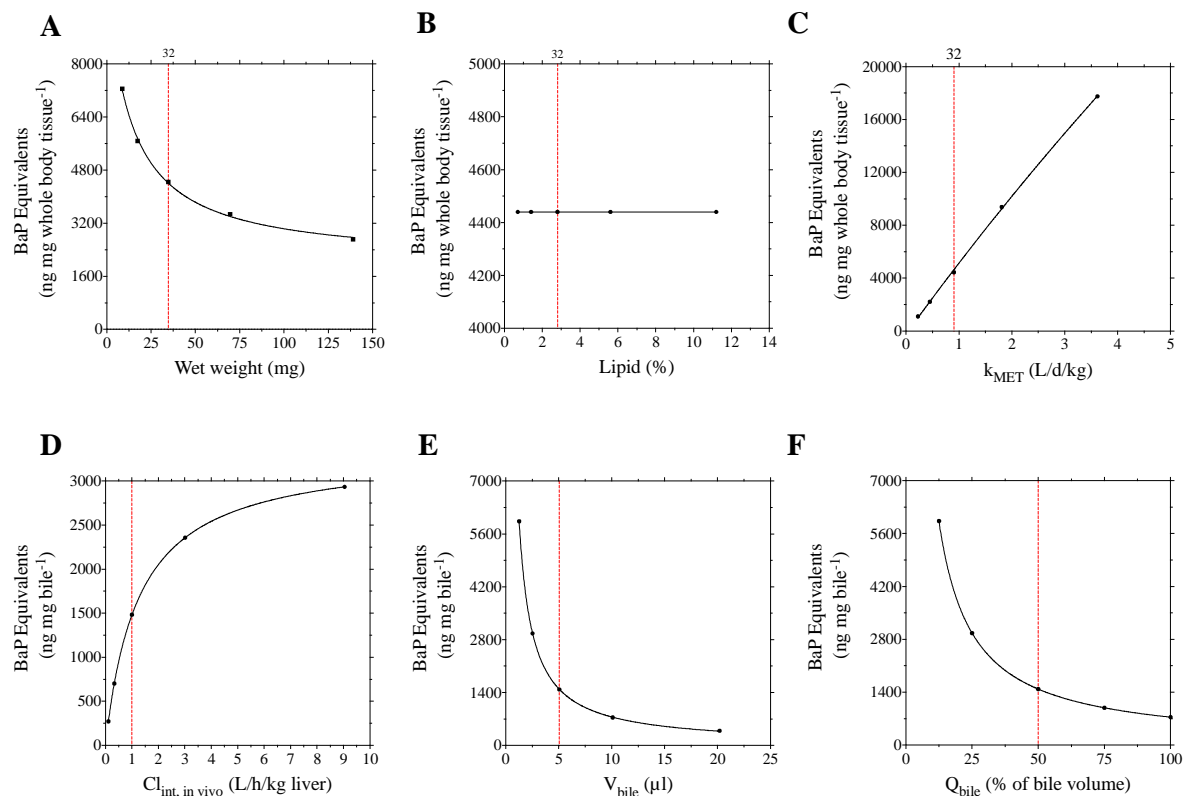
Figure S2. Sensitivity analyses conducted for the ELS one-compartment model (run using the 4.55 µg B[*a*]P/L treatment) and the adult multi-compartment PBTK model (run using the 1.34 µg B[*a*]P/L treatment). The parameters wet weight (A), total lipid content (B) and biotransformation rate (k_{MET}; C) were analyzed for the ELS one-compartment model while the parameters *in vivo* intrinsic clearance ($Cl_{int, in vivo}$; D), bile volume (V_{bile}; E), and bile flow (Q_{bile}; F) were analyzed for the adult multi-compartment model. Model default values are denoted by a red dotted line. For the ELS one-compartment model, the default value is shown for 32 dpf, however a value for zero, three, seven, and 14 dpf was also implemented for each parameter.

12. References

Arnot, J. A., & Gobas, F. A. (2004). A food web bioaccumulation model for organic chemicals in aquatic ecosystems. *Environmental Toxicology and Chemistry: An International Journal*, *23*(10), 2343-2355. DOI 10.1897/03-438

Beach, J. B., Pellizzari, E., Keever, J. T., & Ellis, L. (2000). Determination of benzo [a] pyrene and other polycyclic aromatic hydrocarbons (PAHs) at trace levels in human tissues. *Journal of analytical toxicology*, *24*(8), 670-677. DOI 10.1093/jat/24.8.670

Brinkmann, M., Schlechtriem, C., Reininghaus, M., Eichbaum, K., Buchinger, S., Reifferscheid, G., ... & Preuss, T. G. (2016). Cross-species extrapolation of uptake and disposition of neutral organic chemicals in fish using a multispecies physiologically-based toxicokinetic model framework. *Environmental science & technology*, *50*(4), 1914-1923. DOI 10.1016/j.aquatox.2014.03.021

Debruyn, A. M., & Gobas, F. A. (2007). The sorptive capacity of animal protein. *Environmental Toxicology and Chemistry: An International Journal*, *26*(9), 1803-1808. DOI 10.1897/07-016R.1

Habig, W. H., Pabst, M. J., & Jakoby, W. B. (1974). Glutathione S-transferases the first enzymatic step in mercapturic acid formation. *Journal of biological Chemistry*, *249*(22), 7130-7139.

Kennedy, S. W., & Jones, S. P. (1994). Simultaneous measurement of cytochrome P4501A catalytic activity and total protein concentration with a fluorescence plate reader. *Analytical biochemistry*, *222*(1), 217-223. DOI 10.1006/abio.1994.1476

Lu, Y., Ludsin, S. A., Fanslow, D. L., & Pothoven, S. A. (2008). Comparison of three microquantity techniques for measuring total lipids in fish. *Canadian Journal of Fisheries and Aquatic Sciences*, *65*(10), 2233-2241. DOI 10.1139/F08-135

Lu, D., Harvey, R. G., Blair, I. A., & Penning, T. M. (2011). Quantitation of benzo [a] pyrene metabolic profiles in human bronchoalveolar (H358) cells by stable isotope dilution liquid chromatography–atmospheric pressure chemical ionization mass spectrometry. *Chemical research in toxicology*, *24*(11), 1905-1914. DOI 10.1021/tx2002614

Nichols, J. W., Fitzsimmons, P. N., & Burkhard, L. P. (2007). In vitro-in vivo extrapolation of quantitative hepatic biotransformation data for fish. II. Modeled effects on chemical bioaccumulation. *Environmental Toxicology and Chemistry*, *26*(6), 1304-1319. DOI 10.1897/06-259R.1

OECD (2012), *Test No. 229: Fish Short Term Reproduction Assay*, OECD Guidelines for the Testing of Chemicals, Section 2, OECD Publishing, Paris. DOI 10.1787/9789264185265-en

OECD (2013), *Test No. 210: Fish, Early-life Stage Toxicity Test*, OECD Guidelines for the Testing of Chemicals, Section 2, OECD Publishing, Paris, Paris. DOI 10.1787/9789264070103-en

OECD (2018), *Test No. 319B: Determination of in vitro intrinsic clearance using rainbow trout liver S9 sub-cellular fraction (RT-S9)*, OECD Guidelines for the Testing of Chemicals, Section 3, OECD Publishing, Paris. DOI 10.1787/9789264303232-e

Richardson, S.J, Bai, A., A Kulkarni, A., & F Moghaddam, M. (2016). Efficiency in drug discovery: liver S9 fraction assay as a screen for metabolic stability. *Drug Metabolism Letters*, *10*(2), 83-90. DOI 10.2174/1872312810666160223121836

Stadnicka, J., Schirmer, K., & Ashauer, R. (2012). Predicting concentrations of organic chemicals in fish by using toxicokinetic models. *Environmental science & technology*, *46*(6), 3273-3280. DOI 10.1021/es2043728

Tang, C., Tan, J., Fan, R., Zhao, B., Tang, C., Ou, W., ... & Peng, X. (2016). Quasi-targeted analysis of hydroxylation-related metabolites of polycyclic aromatic hydrocarbons in human urine by liquid chromatography–mass spectrometry. *Journal of Chromatography A*, *1461*, 59-69. DOI 10.1016/j.chroma.2016.07.05

Zhu, S., Li, L., Thornton, C., Carvalho, P., Avery, B. A., & Willett, K. L. (2008). Simultaneous determination of benzo [a] pyrene and eight of its metabolites in Fundulus heroclitus bile using ultra-performance liquid chromatography with mass spectrometry. *Journal of Chromatography B*, *863*(1), 141-149. DOI 10.1016/j.jchromb.2008.01.018